International Journal of Innovative Research and Scientific Studies, 8(8) 2025, pages: 33-54

IJIRSS
International Journal of Innovative Research & Scientific Studies

ISSN: 2617-6548

URL: www.ijirss.com

Comparison between organic solar cells and perovskite photovoltaic cells: Minireview

Soon Min[1*], Md. Hojaifa Daiyan Chowdhury[2], Muhammad Rashique Hamjah Chowdhury[3], Md. Iqbal Bahar Chowdhury[4]

[1]*Faculty of Health and Life Sciences, INTI International University, Putra Nilai, 71800, Negeri Sembilan, Malaysia.*
[2,3,4]*School of Science and Engineering, United International University, Dhaka, Bangladesh.*

Corresponding author: Soon Min (*Email: soonmin.ho@newinti.edu.my*)

Abstract

The photophysics, working principles of organic and perovskite solar cells, the main two photovoltaic technologies that received more attention from the scientific community in recent years are analyzed. For this, the current review focuses on connecting the intrinsic structural (such as crystalline, ionicity) as well as electronic (relative permittivity, binding energy) and optical (absorption coefficient) properties of these organic/perovskite photoactive layers to unveil deep understanding into charging carrier dynamics and recombination kinetics while establishing their relationship with film in tandem with device performance metrics. The review offers insight into the limitations related to both types of solar technologies that are hindering their performance & proposed succinct chart of remedies to cope up with them appropriately causing this bottleneck.

Keywords: Energy consumption, Energy efficiency, Organic solar cells, Perovskite photovoltaic cells, Thin films.

DOI: 10.53894/ijirss.v8i8.10543
Funding: This research work was supported by INTI International University (Ho SM).
History: Received: 13 August 2025 / **Revised:** 15 September 2025 / **Accepted:** 18 September 2025 / **Published:** 7 October 2025

Competing Interests: The authors declare that they have no competing interests.
Authors' Contributions: All authors contributed equally to the conception and design of the study. All authors have read and agreed to the published version of the manuscript.
Transparency: The authors confirm that the manuscript is an honest, accurate, and transparent account of the study; that no vital features of the study have been omitted; and that any discrepancies from the study as planned have been explained. This study followed all ethical practices during writing.
Publisher: Innovative Research Publishing

1. Introduction

The sun is an abundant source of energy, delivering approximately four million exajoules to the Earth's surface each year. This vast energy potential positions solar energy as one of the safest and most plentiful resources available [1]. In fact, the amount of solar energy received in just one hour exceeds the total energy consumed by humanity in an entire year. Harnessing this resource through photovoltaic cells has emerged as a crucial strategy in the fight against climate change and the reduction of carbon footprints.

As of 2021, the global installed capacity of solar panels reached an impressive 866 gigawatts (GW), accounting for 28% of the world's total energy capacity. Projections indicate that by 2050, this figure could soar to over 4500 GW, driven by advancements in photovoltaic technology that offer practicality, longevity, and reduced maintenance costs. The

increasing integration of solar solutions into urban environments, particularly through building-applied and building-integrated photovoltaic systems [2], further underscores the potential for solar energy in modern infrastructure.

Photovoltaic technology has evolved through distinct generations. The first generation primarily utilizes crystalline silicon [3], while the second generation incorporates thin films made from amorphous and polycrystalline semiconductors such as cadmium telluride, copper indium gallium selenide, and gallium arsenide. Currently, the third generation is emerging, characterized by rapid development and promising alternatives that aim to reduce costs and operating temperatures.

Among the forefront of this innovation are organic solar cells and perovskite solar cells, which utilize solution-processable semiconductors. Unlike traditional silicon-based solar cells that rely on expensive [4], high-purity silicon produced at high temperatures, these new technologies leverage low-energy manufacturing processes, such as roll-to-roll printing. This method not only lowers production costs but also enhances scalability. Furthermore, organic and perovskite materials boast a significantly higher absorption coefficient—greater than 10^5 cm^{-1} compared to silicon's 10^3–10^4 cm^{-1} in the visible spectrum. This property allows for reduced material usage, making them lighter and more economical.

Interestingly, at lower levels of solar irradiation, organic and perovskite solar cells demonstrate enhanced power conversion efficiency, while traditional silicon cells tend to perform less effectively. This characteristic makes organic and perovskite technologies particularly suited for indoor energy harvesting applications [5]. Additionally, their ability to be fabricated on flexible substrates opens new avenues for portable and wearable electronics.

Recent research has identified optimal applications for these technologies: organic solar cells are favoured for indoor settings and Internet of Things devices, while perovskite solar cells are increasingly being integrated into building structures—such as windows, walls, and roofing materials—offering aesthetic and functional benefits to modern architecture [6].

This article aims to review the properties of photoactive materials used in organic and perovskite solar cells, employing various analytical techniques. The photovoltaic parameters of both cell types will be discussed comprehensively, alongside strategies for enhancing solar cell performance. As we continue to innovate and adapt to new technologies, the future of solar energy promises to be as bright as the sun itself.

2. Experimental

To identify English-language articles about the solar harvesting, the search was performed by the authors in the library on the related journals from 2020 to 2025. The databases that we searched were Google Scholar, Taylor & Francis, ACS, Scopus, Wiley Online Library, Science Direct, and MDPI. The search terms were the "organic solar cells", “absorption properties”, "silicon based solar cells", "thin film based solar cells", “chalcogenide thin films”, "perovskite solar cells", "band gap”, “semiconductor materials”, and “photovoltaic parameters”.

3. Literature Survey

Organic solar cells are a unique form of solar technology that use organic semiconductors to absorb light and convert it into electricity. Unlike traditional silicon solar cells, these organics are flexible: they’re so light you can pick them up, and they can be produced by printing, which could cut costs massively [7]. Organic solar cells have an active layer made of certain organic materials (polymers or small molecules) that have the property of absorbing light efficiently and permitting the efficient production of electricity. When it absorbs sunlight, the energy from the sunlight stimulates electrons, generating "excitons," which are coupled with electrons and holes. For the excitons to get separated into free charge carriers, that is electrons and holes, electricity should be generated. For a better separation of excitons, most organic solar cells contain a mixture of electron donor and electron acceptor materials.

Perovskite photovoltaic devices are a type of thin-film technology, which is being developed to convert sunlight into electricity using light absorbing material based on a perovskite crystal structure, known for its unique light absorption and electronic emission properties. The cells are an attractive development in solar technology because of their high potential efficiency, which also carries a low production cost. In solar cells, perovskites are a class of materials that share a certain crystal structure [8]. Often, they are organic-inorganic halide materials with extraordinary efficiency converting solar energy and light to electrical power. When sunlight hits the perovskite layer, it generates excitement in the electrons that form in the material, known as electron-hole pairs. These pairs are then split, with electrons pooling into the electron transport layer and the holes the hole transport layer. The charged particles are then collected by electrodes and used to produce an electrical current by which a variety of electrical devices may be energized.

3.1. Structure of organic solar cells and perovskite photovoltaic cells

The architectural designs of organic solar cells and perovskite solar cells exhibit notable similarities, particularly concerning their charge transport layers (CTL) and metallic contacts. However, the key distinction resides in the materials utilized for the photoactive layer. Organic solar cells predominantly rely on conjugated polymers or derivatives of fullerene/non-fullerene, whereas their perovskite counterparts utilize perovskite materials.

Organic solar cells, characterized by their conjugate polymer technology, represent a burgeoning segment of third-generation solar technology [9]. Their appeal lies in several advantageous properties: the use of low-cost materials, the potential for solution-based processing, economical manufacturing techniques, and their semi-transparent, flexible, and lightweight design. Initially, the efficiency of organic solar cells was below 1%; however, advancements in technology have propelled this figure to exceed 18%, reflecting significant progress in device architecture, material design, and morphology.

The structural configurations of organic solar cells can be classified into three main categories: bi-layer (BL), single-layer (SL), and bulk heterojunction (BHJ), which includes both regular (n-i-p) and inverted (p-in) designs. In the realm of organic solar cells [10], the built-in electric field (E_bi) results from the work function disparities between electrodes, facilitating the separation of excitons generated in the photoactive layer. This layer is typically sandwiched between the electrodes. These utilize a solitary organic semiconductor, which results in low power conversion efficiency (about 0.1%) for p-phenylene vinylene-based organic solar cells.

In terms of bilayer cells, these cells employ a heterojunction of electron donor and acceptor (D/A). The excitons generated here can be separated into electron-hole pairs, leading to improved efficiencies over single-layer designs [11]. Nevertheless, the efficiency is still hampered by the short diffusion lengths of conjugated polymers, which range from 4-20 nm, causing recombination as they approach their respective electrodes.

In relation to bulk heterojunction cells, this configuration utilizes a blend of donor and acceptor materials, which enhances the diffusion length and, consequently, the power conversion efficiency. To further boost efficiency within the n-i-p structure, charge transport layers are employed to minimize recombination near the electrodes. The electron transport layer facilitates electron movement while blocking hole transport, and vice versa for the hole transport layer.

Despite these advancements, a significant challenge remains in the production of organic solar cells [12]. The requirement for vacuum processing when placing the cathode atop the photoactive layer hinders the full realization of solution-based processing, creating a bottleneck for large-scale manufacturing. To mitigate this issue, it is often necessary to transition from a regular bulk heterojunction structure to an inverted one, which circumvents the vacuum steps and enables fully solution-processed production on a larger scale.

The evolution of perovskite semiconductor-based solar cells has positioned them as the fastest-growing technology in the realm of third-generation solar solutions [13]. Since their introduction in 2009, power conversion efficiencies have soared dramatically, increasing from a mere 3.8% to an impressive 25.73%. This remarkable enhancement can be attributed to the unique structural, electronic, and optical properties inherent to perovskite materials.

Perovskite solar cells are primarily divided into two categories: mesoscopic and planar. Each category can further be classified into regular n-i-p and inverted p-i-n structures. In terms of mesoscopic structure, this configuration typically includes a metal anode, a hole transport layer, a photoactive perovskite layer, a thin mesoporous layer (such as TiO_2 or Al_2O_3), and a transparent conductive cathode [14]. This structure, while requiring high-temperature processing, enhances film quality and morphology control, which is critical for device reliability.

In related to planar structure**,** the planar structure omits the mesoporous layer. This design simplifies fabrication, particularly suitable for flexible solar panels, although it may compromise some aspects of film quality [15]. The hole transport layer in these cells plays a pivotal role in mitigating interfacial charge recombination, thereby improving charge collection and enhancing both open circuit voltage and overall efficiency. The performance disparities between organic and perovskite solar cells can largely be attributed to the intrinsic material properties.

Organic semiconductors, primarily composed of carbon and hydrogen, exhibit a crystalline structure often categorized as monoclinic or triclinic. They are generally classified into conjugated polymers and small molecules, depending on their molecular weight. Conjugated polymers can be prepared through solution processes, while small molecules are typically deposited via thermal evaporation. Conversely, perovskite semiconductors, often derived from the mineral $CaTiO_3$, follow a general chemical formula of ABX_3. Here, the A-site is filled with larger monovalent cations like methylammonium or caesium, while the B-site is occupied by smaller divalent metallic cations such as lead or tin, and the X-site is represented by halide anions.

The fundamental distinctions between organic solar cells and perovskite solar cells lie in their structural bonding and electronic properties. Organic solar cells, characterized by weaker van der Waals forces, tend to exhibit softer material properties. In contrast, perovskite materials serve as direct band-gap semiconductors [16], facilitating superior charge transport capabilities. The dielectric constant of organic semiconductors is significantly lower (εr=2-4) compared to that of perovskites (εr=20-50), which leads to stronger electron-hole interactions in organic materials. This results in the formation of tightly bound electron-hole pairs, whereas perovskites exhibit weakly-bound excitons.

Perovskite solar cells demonstrate a substantially higher effective carrier mobility [17], ranging from 0.1 to 10 $cm^2/V \cdot s$, which is approximately 1,000 times greater than the mobility observed in conjugated polymers. This is attributed to the dominant band-like transport mechanism in perovskites, in contrast to the hopping transport seen in organic semiconductors. Furthermore, the effective carrier lifetime in perovskite solar cells is also notably higher [18], suggesting a significantly faster bimolecular recombination rate compared to organic counterparts. The resulting effective mobility-lifetime product in perovskite cells is larger, indicating a more efficient charge extraction mechanism, even though diffusion transport in thicker active layers.

3.2. Intrinsic Properties of Photoactive Materials

Organic semiconductors, primarily composed of carbon and hydrogen atoms, are intricately structured through relatively weak van der Waals bonds. These materials typically crystallize in monoclinic or triclinic forms [19]. They can be classified into two main categories based on molecular weight: conjugated polymers and small molecules. Conjugated polymers exhibit a range of molecular weights, while small molecules possess precise, defined weights. The fabrication methods for these organic semiconductors vary; conjugated polymers are often prepared through solution processes, whereas small molecules are typically deposited via thermal evaporation, although solution processing can also be adapted for their development.

Perovskite semiconductors derive their name from the mineral $CaTiO_3$ and are characterized by a general chemical formula of ABX_3. In this structure, the 'A' site is filled with large-radius, monovalent cations. The 'B' site is occupied by smaller, divalent cations, while the 'X' site includes monovalent halide anions (Cl^-, Br^-, or I^-). Depending on their crystal structure, the resulting crystal structure can be cubic, tetragonal, or orthorhombic.

The inherent softness of organic semiconductors, particularly conjugated polymers [20], stems from their weaker van der Waals bonding. In contrast, perovskites are often categorized as direct band-gap semiconductors. When comparing the two, thin films of conjugated polymers tend to exhibit lower crystallinity and ionic character. This is reflected in their dielectric constant, which ranges from 2 to 4, significantly lower than that of perovskites, which can span from 20 to 50. Consequently, the Coulombic interactions between electrons and holes in conjugated polymers are stronger relative to those in perovskites.

The process of photoexcitation in these materials leads to the formation of electron-hole pairs, referred to as Frenkel excitons in organic semiconductors due to their lower dielectric constants. In contrast, perovskite semiconductors generate Wannier–Mott excitons, characterized by their relatively weak binding. For pure films of conjugated polymers, the Frenkel excitons have shorter lifetimes—ranging from approximately 20 picoseconds to 1 nanosecond—and limited diffusion lengths between 3 and 20 nanometers. Additionally, the stronger electron-phonon coupling in organic semiconductors results in a greater variety of phonon modes and excited states compared to their perovskite counterparts. Structural and energetic disorders are also more pronounced in conjugated polymers, leading to increased localization of excited states.

The effective carrier mobility in perovskite semiconductors can range from 0.1 to 10 $cm^2/V{\cdot}s$, which is roughly 1,000 times greater than the mobility observed in organic semiconductors [21], typically between 10^{-5} and 10^{-4} $cm^2/V{\cdot}s$. This enhanced mobility in perovskites is attributed to dominant band-like transport mechanisms and low effective mass, facilitating efficient charge carrier movement. Conversely, organic semiconductors rely on hopping-like transport mechanisms involving small polarons, which inherently limit their mobility.

Recent studies have shed light on the remarkable properties of perovskite solar cells, particularly emphasizing their superior performance over traditional organic semiconductor-based solar cells. One of the key findings is that the effective carrier lifetime (τ) in perovskite solar cells is significantly enhanced, exhibiting a 1-2 order of magnitude increase compared to the lifetimes observed in organic solar cells. This translates to a bimolecular recombination rate in perovskite solar cells that is 10 to 100 times faster than that found in organic solar cells [22].

The exceptional performance of perovskite solar cells largely be attributed to their higher relative permittivity (εr), which exceeds 25, in stark contrast to the relative permittivity values of organic semiconductors that hover around 2 to 4. This substantial difference in dielectric properties leads to a lower Coulomb capture radius for bimolecular recombination in perovskite solar cells, which is approximately 1 to 2 orders of magnitude smaller than that of organic solar cells. Here, the Coulomb capture radius is defined by the equation that incorporates the relative permittivity of the material, the elementary charge, the Boltzmann constant, and absolute temperature.

$$r_C = \sqrt{\frac{q^2}{4\pi\varepsilon_0\varepsilon_r kT}} \qquad (1)$$

where ε_r (ε_0) is the relative permittivity of material (vacuum), with (q, k, T) being the (elementary charge, Boltzmann constant, absolute temperature). The bimolecular recombination lifetime in organic solar cells can range from 1 to 100 microseconds, which is consistent with their relatively larger Coulomb capture radius (rc) values (rc, organic solar cells>15 nm) compared to those of perovskites (rc, perovskite solar cell<2 nm). This stark contrast underscores the efficient charge carrier dynamics present in perovskite solar cells.

The dielectric screening effect observed in perovskite solar cells is attributed to their more ionic character and the local ferroelectric phenomena inherent in the perovskite structure. These attributes not only enhance the material's ability to manage charge carriers but also contribute to improved overall efficiency.

Another significant advantage of perovskite solar cell is their effective carrier mobility-lifetime product ($\mu\tau$), which is markedly larger than that of organic solar cells. With mobility (μ) being approximately 1,000 times greater and the effective lifetime (τ) being 10 to 100 times shorter than those found in organic semiconductors, perovskite solar cells benefit from an increased carrier diffusion length. This enhancement allows for efficient charge extraction, even in thicker active layers, driven solely by diffusion transport.

3.3. Optical Properties of These Solar Cells

Organic solar cells and perovskite solar cells both exhibit remarkable potential for effective light absorption across the solar spectrum, particularly within the visible to near-infrared range [23]. This capability is largely attributed to their thin active layers, which typically range from 100 to 500 nanometres, and their high absorption coefficients, often exceeding 10^5 cm^{-1}.

The absorption profiles of these two technologies reveal distinct advantages. Organic blends tend to display enhanced absorption in the visible and near-infrared spectrum, making them particularly effective for harvesting solar energy in these wavelengths. In contrast, perovskite materials excel in the blue and ultraviolet regions, showcasing their versatility and capacity for energy conversion.

In the pursuit of achieving high power conversion efficiencies in bulk heterojunction organic solar cells, it is crucial to maintain an active layer thickness at or below 100 nanometres. Thicknesses exceeding this threshold can lead to increased recombination losses, ultimately hindering the overall efficiency of the device. Conversely, perovskite solar cells exhibit a

different trend [24]; they thrive with thicker active layers, often greater than 500 nanometres. This is largely due to their superior carrier mobility, which facilitates more efficient charge extraction, thereby enhancing efficiency.

The contrasting photophysical mechanisms at play in organic solar cells and perovskite solar cells underscore the importance of tact in optimizing solar cell performance. For organic solar cells, the effective limit for tact is approximately 100 nanometres, while perovskite solar cells can operate efficiently within a broader range of 200 to 700 nanometres. This divergence in operational parameters highlights the unique characteristics of each technology and their respective approaches to maximizing solar energy absorption and conversion.

The photoluminescence (PL) quenching is a simple assay to measure the charge-transfer yields (Table 1) between the donor and acceptor materials in organic solar cells and between the perovskite/ charge transport layers materials in perovskite solar cells. In organic solar cells, photoluminescence emission occurs from Frenkel excitons; in perovskite solar cells, this is from radiative bimolecular recombination of unbound charges [25]. Enhanced exciton/phonon coupling due to increased phonon modes and localized excited states causes photoluminescence-broadening in organic solar cells [26], whereas low energy disorder of radiative states causes photoluminescence-narrowing in perovskite solar cells. Optimal photoluminescence emission quantum yield in organic solar cells depends on the material selection (film processing). However, absolute photoluminescence quantum yields in both organic solar cells and perovskite solar cells is <10% [27]. In organic solar cells, the stronger photoluminescence quenching comes from the donor and acceptor blends and depends on how exciton dissociation is counteracted by the nonradiative recombination at the donor and acceptor interface [28], whereas the same in perovskite solar cells comes from charge transport layers and depends on the irradiation intensity [29]. The dominance of nonradiative recombination over radiative recombination in organic solar cells leads to their lower electroluminescence yields; the opposite dominance observed in perovskite solar cells results in higher electroluminescence yields.

Table 1.
Photoluminescence (PL) quenching.

	OSC	**PSC**
Origin of PL emission	mostly from Frenkel excitons	from radiative bimolecular recombination of unbound charges
PL broadening	wider due to enhanced exciton/phonon coupling	narrower due to the less energetic disorder of the radiative states
Dependency of Optimal PL emission quantum yield	on material selection	on processing
Absolute PL quantum yields	< 10%	< 10%
Stronger PL quenching	comes from the D/A blends	comes from CTLs
Electroluminescence yields	Lower	Higher

3.4. Charge Carrier Dynamics of Organic Solar Cells and Perovskite Photovoltaic Cells

Intrinsic properties of photo active layers used in organic solar cells and perovskite solar cells are strongly linked with their charge carrier dynamics (generation, separation, transport, and recombination of charge carriers) and hence, impact significantly on their photovoltaic performance. The effects of these intrinsic properties on the generation, separation, and transport are briefed in Table 2, whereas the effects on recombination kinetics are manifested in Table 3. The details of these processes are discussed as follows.

Table 2.
Photo-induced Charge generation.

	OSC	**PSC**
Exciton generation and separation	rigidly-bound Frenkel excitons are generated the dissociation of which requires a D/A interface.	weakly-bound Wannier–Mott excitons are generated which immediately dissociated into free charge carriers.
Charge transport	hopping-like and is associated with small polaron motion.	band-like and is associated with a small effective mass of charge carriers.

Table 3.
Properties associated with recombination kinetics of OSC and PSC.

	OSC	**PSC**
Bimolecular recombination rate	slower due to smaller capture cross section for lower dielectric constant	faster due to larger capture cross section for higher dielectric constant.
Carrier lifetime	shorter due to less charge carrier delocalization and higher electron/phonon coupling	longer due to higher carrier delocalization and less electron/phonon coupling
$\mu\tau$ product	smaller, so charge extraction is less efficient	larger and hence, charge extraction is efficient in thicker photoactive layers
Trap-state density	Higher	Lower

The lower ε_r and the stronger exciton/charge localization result in higher exciton binding energy (E_b) in conjugated polymers (CPs) (> 100 meV) than in perovskites (< 25 meV), as binding energy is inversely related to ε_r as [30])-

$$E_b = \frac{q^2}{4\pi\varepsilon_0\varepsilon_r R} \quad (2)$$

where R is the mean electron–hole distance. The higher binding energy in conjugated polymers results in large electron-hole Coulombic attraction and hence, an offset energy (ΔE) is needed to dissociate the rigidly bound Frenkel excitons (FEs) by charge transfer (CT) at the donor and acceptor interface. An appropriately chosen bulk heterojunction structure can provide the required offset energy.

In perovskite solar cells, due to lower binding energy of perovskite films, the electron-hole Coulombic interaction is poor for the photogenerated weakly-bound Wannier–Mott excitons. These Wannier–Mott excitons, therefore, are short-lived and immediately dissociated into free charge carriers. In other words, photoexcitation in perovskite films like any inorganic semiconductor directly generates free charge carriers.

The harvesting of solar energy in bulk heterojunction organic solar cells is associated with four fundamental processes [31]: (i) Frenkel excitons generation by light absorption, (ii) Frenkel excitons diffusion to the donor and acceptor interface (iii) two- step Frenkel excitons dissociation at the donor and acceptor interface: charge transfer states (polaron pairs) creation followed by their dissociation into free charge carriers and (iv) transportation and collection of charge carriers. The offset energy required in process (iii), depends on the electronic energy levels of donor and acceptor materials (HOMO- highest occupied molecular orbital) and LUMO- lowest unoccupied molecular orbital) and can be evaluated as $\Delta E_{HOMO} = HOMO_D - HOMO_A$ or $\Delta E_{LUMO} = LUMO_D - LUMO_A$.

A large offset energy suppresses the recombination loss of the charge transfer states and reduces both the electronic and optical band gap of the blend. The band gap reduction reduces the open circuit voltage due to increased voltage loss due to enhanced photon absorption. Therefore, a well-judged compromise between open circuit voltage and short circuit current sets the offset energy requirement, which applies a fundamental limit on the organic solar cells' efficiency; such limit is not applicable for perovskite solar cells.

Recombination mechanisms are very crucial to achieving high efficiency of organic solar cells and perovskite solar cells, as these mechanisms determine the charge extraction efficiency and open circuit voltage of these cells. In both organic solar cells and perovskite solar cells, recombination kinetics usually include radiative and nonradiative recombination mechanisms. However, lower photoluminescence quantum yields (<10%) reported for most organic solar cells and perovskite solar cells imply that the dominant recombination mechanism in these cells is of nonradiative type. Surface recombination at the active layer/contact interface also needs to be considered in these cells, which is particularly critical for perovskite solar cells.

Based on Shockley–Queisser detailed balance model, $V_{loss} = \frac{E_g}{q} - V_{OC}$, where E_g is the material bandgap, consists of three components as-

$$V_{loss} = \Delta V_{OC}^{SQ} + \Delta V_{OC}^{rad} + \Delta V_{OC}^{non-rad} \quad (3)$$

Where,

- The component ΔV_{OC}^{SQ} corresponds to the portion of V_{loss} that depends on E_{gopt} under standard operating conditions and is 0.25-0.30 eV for an ideal semiconductor.
- The component ΔV_{OC}^{rad} accounts for the V_{loss} for a realistic device due to the absorption below E_{gopt}; the extra transitions provided by the sub-band gap states extends absorption to lower energy region thereby reducing achievable open circuit voltage.
- The component $\Delta V_{OC}^{non-rad}$ is the V_{loss} due to nonradiative recombination of charge transfer states and can be approximately expressed as follows [32]-

$$\Delta V_{OC}^{non-rad} = -\frac{kT}{q} ln(EQE_{EL}) \quad (4)$$

$$EQE_{EL} = \frac{k_r}{k_r + k_{nr}} \quad (5)$$

with EQE_{EL} and k_r (k_{nr}) being electroluminescence external quantum efficiency and radiative (non-radiative) rate respectively. $V_{OC}^{non-rad}$ is the most dominant component of V_{loss} in organic solar cells.

High photocurrent organic solar cells exhibit greater V_{loss} than perovskite solar cells (0.5-0.7 V as compared to 0.34 V for perovskite solar cells), resulting in lower open circuit voltage and fill factor than perovskite solar cells [33]. This higher energy loss in organic solar cells can be attributed to the higher energy loss in forming polarons and to the higher recombination loss due to the reversible (irreversible) charge trapping by the shallow (deep) trap states present in the photoactive material.

The recombination associated with the trap states, termed as bimolecular recombination is crucial in both organic solar cells and perovskite solar cells and depends strongly on the trap-state density. In organic solar cells, the trap-state density is higher and is due to the lower crystallinity, structural distortion/inhomogeneity, and various molecular level defects; in perovskite solar cells, the relatively lower trap-state density is due to surface/grain boundaries type crystal defects [34]. To control trap-state density, organic solar cells require molecular-level design and purification [35], whereas perovskite solar cells require passivation of surface/grain boundaries and optimized film fabrication techniques [36].

To achieve lower V_{loss} and hence, the higher open circuit voltage (> 1 V) for organic solar cells, the donor and acceptor energy levels can be tuned to increase E_{gopt}, however, at the expense of lower short circuit density. Therefore, a compromise of optimum short circuit current and high open circuit voltage is required in organic solar cells, which is not required in perovskite solar cells.

Owing to lower carrier mobility (μ) in the photoactive layer, hopping like charge transport is observed in organic solar cells. In organic solar cells, the charge transport is associated with small polaron motion [37], whereas the same is associated with a small effective mass of charge carriers in perovskite solar cells. Drift type transport drives the free charges to the respective electrode in organic solar cells. In both cells, the difference in work functions between the electrodes develops a built-in field; however, built-in field is screened by the migration of mobile ions in perovskite solar cells. In both cells, electrodes collect the free charges. Charge transport efficiency is mainly limited by the extent to which the charge extraction is compelled by the recombination mechanisms [38].

In addition to the intrinsic material properties of the photoactive layers, the performance metrics of both organic solar cells and perovskite solar cells are strongly affected by the solar irradiation intensity, charge transport layer optimization and photoactive layer thickness. Additionally, in organic solar cells, these metrics are also affected by built-in electric field, and offset energy at the donor and acceptor interface. These functional effects are summarized in Table 4. Power conversion efficiency at lower light intensities in both organic solar cells and perovskite solar cells tends to increase as the charge extraction efficiency is less limited by the bimolecular recombination due to lower carrier density accumulated at lower light intensity [39].

Table 4.
Functional effects of the material properties for OSC and PSC.

		OSC	**PSC**
V_{OC} (V)		≈ 0.6−0.8 ≈ 0.8−1.0 (NFA-based)	≈ 0.9−1.1
V_{loss} (V)		typically, 0.5-0.7	as low as 0.34
PCE at lower light intensities		tends to increase	tends to increase
E_{bi}		Strong	Negligible
Optimizationof transport (HTL and ETL)	Layers	Critical	More critical
Charge transport efficiency		Limited by the extent to which the charge extraction is compelled by the recombination mechanisms	Same as OSC
t_{act} dependency of J_{SC}		J_{SC} decreases as t_{act} increases	J_{SC} is insensitive to t_{act}-variation
t_{act} dependency of FF		For most OSCs with NLF ≈ 10^{-1}, FF (and J_{SC}) decreases for t_{act} > 100 nm; for some blends with NLF ≈ 10^{-3} FF increases for t_{act} > 100 nm.	FF of PSCs is insensitive to $t_{act.}$
ΔE dependency of V_{OC} and J_{SC}		ΔE between D/A is critical for OSCs. This offset reduces both the electronic and optical bandgap. The former reduction reduced V_{OC}, whereas, the later one increases J_{SC}	Not applicable

Optimization of transport layers (HTL and ETL) is critical for both organic solar cells and perovskite solar cells. To achieve high performance for perovskite solar cells, this optimization is more critical due to their influence on the active layer crystallization and surface trap passivation as well as on the minimization of the surface recombination at the perovskite/transport layer interface.

In organic solar cells, the photoactive layer and thickness has strong effects. Herein short circuit current decreases as thickness increases due to higher built-in electric field screening of the space charge layer which is formed due to unintended doping [40], mismatch of carrier mobility [41], and accumulation of photogenerated charges into tail states [42]. The thickness dependency of fill factor is affected by the non-Langevin factor of photoactive layer that accounts for how slower the bimolecular recombination rate is than the same expected for photoactive layer with Langevin behaviour. For most organic solar cells with non-Langevin factor=10^{-1}, fill factor (and short circuit current) decreases for thickness more than 100 nm; for some blends (P3HT:$PC_{61}BM$ and BTR: $PC_{71}BM$) with non-Langevin factor about 10^{-3} fill factor increases for thickness greater than 100 nm. However, both short circuit current and fill factor are insensitive to thickness variation due to higher carrier mobility and higher $\mu\tau$ product for which charges are extracted efficiently in thicker perovskite solar cells where charge transport is only diffusion type.

3.5. Progress in BHJ OSCs Toward High PCE

To achieve high efficiency for bulk heterojunction organic solar cells, the donor and acceptor materials should have (i) complementary and stronger absorption in the visible/IR range of the solar spectrum to increase short circuit current (ii) appropriate HUMO-LOMO level alignment to increase open circuit voltage (iii) optimized donor and acceptor phase separation, blend morphology and crystallinity for enhanced short circuit current and fill factor and (iv) higher mobility of the charge carriers [43]. Therefore, intensive research efforts have been continuously carried out in the design and synthesis of novel donor and acceptor materials with these traits. In the following subsections, the progress in bulk heterojunction organic solar cells has been described.

3.5.1. Fullerene Derivative-based Acceptors (FDAs)

The discovery of polymer-to-fullerene transfer of photogenerated electrons [44], boosted the use of soluble fullerene derivatives. Since then, the blend of fullerene derivative-based acceptor (FDAs) such as $PC_{61}BM$ and $PC_{75}BM$ with conjugate polymer donors (CPDs) such as P3HT are widely used for their increased donor and acceptor interface to separate the excitons efficiently. Power conversion efficiency of 4.37% [45] and 4.1% [46] are reported with $PC_{61}BM$:P3HT and $PC_{71}BM$:P3HT blends. Continuous efforts to increase efficiency made by the researchers put forward the use of alternative fullerene derivatives such as $NC_{61}BM$ [47], $bisPC_{61}BM$ [48], F [49], F1 [50], ICBA [51, 52] and $IC_{70}BA$ [53]. The increase in LUMO level w.r.t. $PC_{61}BM$ ($PC_{71}BM$) observed in these alternatives increases the open circuit voltage and power conversion efficiency. Figures 1(A, B) show the increase in open circuit voltage and efficiency of some selected bulk heterojunction organic solar cells that employed different fullerene derivative -based acceptors with P3HT polymer doner.

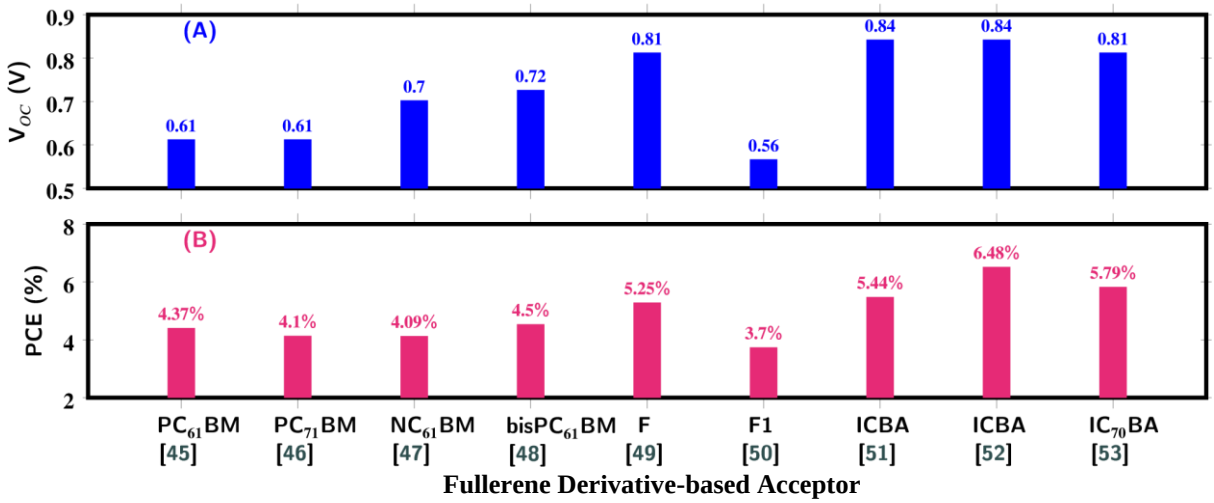

Figure 1.
(A) open circuit voltage and (B) power conversion efficiency of selected bulk heterojunction organic solar cells employing blends of different fullerene derivatives and P3HT.
Source: Li, et al. [45];Troshin, et al. [46] Kim, et al. [47]; Lenes, et al. [48], Mikroyannidis, et al. [49], Zhao, et al. [50], He, et al. [51], Zhao, et al. [52] and He, et al. [53]

3.5.2. Narrow-bandgap Polymer Donor (PD) Materials

Polymer donor materials with E_{gopt} > 1.8 eV are wide bandgap with E_{gopt} < 1.6 − 1.8 > eV are medium bandgap and, with E_{gopt} < 1.6 eV are low bandgap materials [31]. Although wide band gap polymer donors (MEH-PPV, MDMO-PPV, and P3HT) are widely used in the early days of organic solar cells, they have issues of absorption-spectra-mismatch with fullerene derivative-based acceptors resulting in low short circuit current and power conversion efficiency. Addressing this mismatch, numbers of medium band gap and lower band gap polymer donors have been explored such as PCPDTBT [54], PTB1 [55], PTB7 [56, 57], PTB7-Th [58, 59], PBDTTT-CF [60], PffBT4T-2OD [61]and PffBT4T-C9C13 [62]. All these narrow bandgap materials, owing to their lower E_{gopt} have stronger absorption, demonstrate higher short circuit current and hence higher efficiency. As seen from Figures 2(A, B), short circuit current=20.2 mA/cm^2 and efficiency=11.7% can be achieved for a bulk heterojunction organic solar cell with PffBT4T-C9C13 based medium band gap polymer donor and $PC_{71}BM$ based fullerene derivative-based acceptors [62].

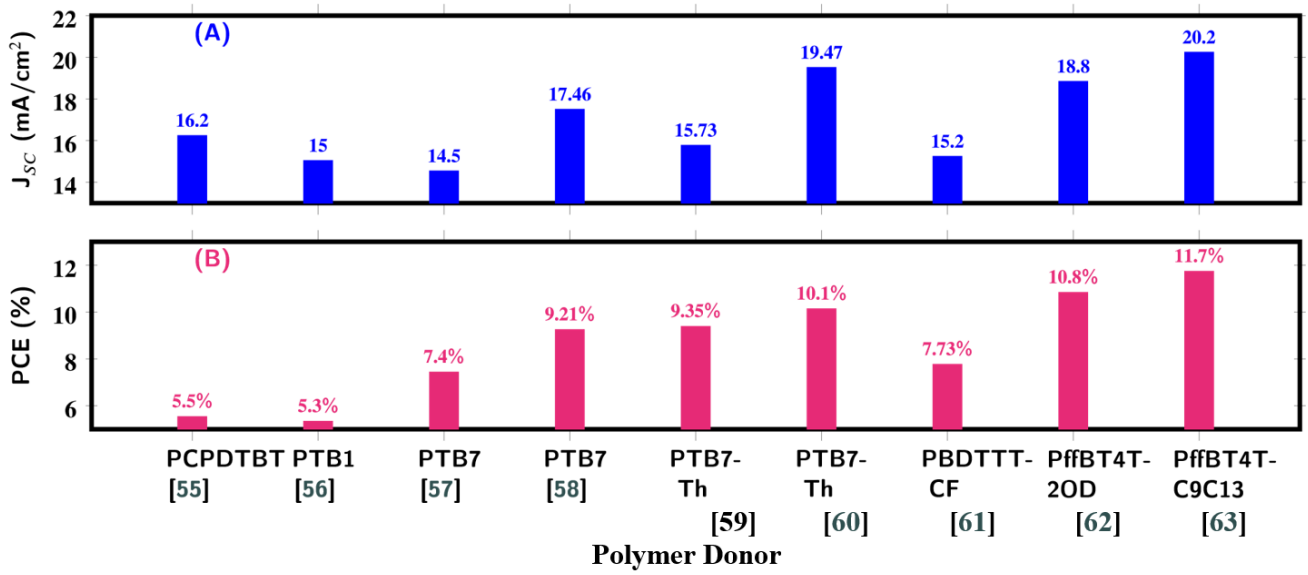

Figure 2.
(A) Short circuit current and (B) power conversion efficiency of selected bulk heterojunction organic solar cells with blends of different polymer donors and $PC_{71}BM$-based Fullerene acceptor.
Source: Peet, et al. [54], Liang, et al. [55], Liang, et al. [56], Chen, et al. [60], Liu, et al. [61], Zhao, et al. [62]

3.5.3. Non-Fullerene Acceptors (NFAs)

The photocurrent in bulk heterojunction organic solar cells can be generated through two mechanisms, namely channel I and channel II [43]. Channel I involves the photoexcitation in donor material followed by the donor-to-electron charge transfer by electrons (related to ΔE_{LUMO}), whereas, channel II associates the photoexcitation in acceptor material followed by the acceptor-to-donor charge transfer by holes (related to ΔE_{HOMO}), as depicted in Figure 3. For fullerene derivative-based acceptor based organic solar cells, channel I mechanism is dominant due to the negligible channel II mechanism associated with their low absorption profile. On the other hand, non-fullerene small molecules and polymers, being narrow bandgap materials, have strong absorbance [43]. Therefore, both channel I and II mechanisms are dominant in NFA-based organic solar cells leading to their higher short circuit current [43, 63]. The tunability of HOMO-LUMO levels of NFA provides better control over their E_g and E_{gopt} [64], yielding enhanced short circuit current and open circuit voltage of NFA-based organic solar cells. Moreover, use of advanced NFA improves environmental stability as compared to FDAs [21].

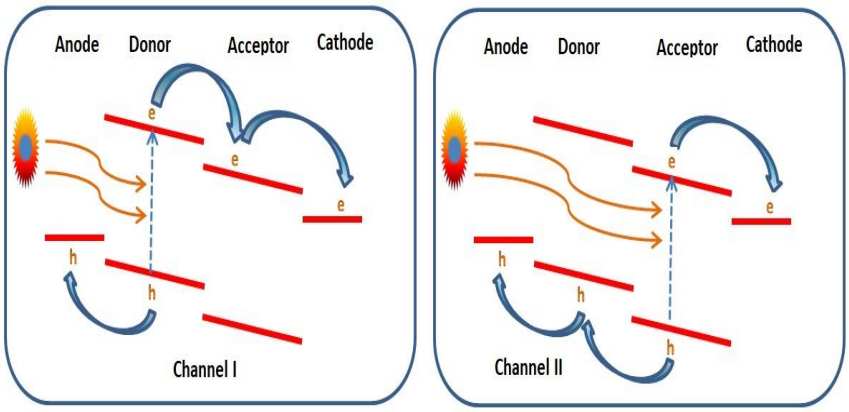

Figure 3.
Channel I and II mechanisms in bulk heterojunction organic solar cells.

3.5.4. Small molecular NFAs

Among various strategies for constructing small molecular non-fullerene acceptors, the most high-performance synthesized template is the push-pull conjugated structure with A-D-A backbone for enhanced conjugation and decreased bandgap, where A is electron-withdrawing, and D is the electron-donating moiety [65]. In addition to the flexible synthesis, the A-D-A backbone-based small molecule non-fullerene acceptors demonstrate an easily tuned absorption spectrum extended to even near-infrared region and an enhanced charge transfer benefitted by the rigid backbone and hence, offer themselves as excellent acceptor materials for bulk heterojunction organic solar cells. In the literature, several small molecular non-fullerene acceptors such as IDIC [66], ITIC [67], IT-4F [68], IOIC3 [69], BTP-4Cl [70], Y6 [71, 72], Y6Se [73], m-BTP-PhC6 [74], BTP-eC9 [75] and L8BO [76] are reported. Plots in Figure 4(A-C) present the photovoltaic properties of device parameters based on some selected small molecular non-fullerene acceptors. As high as 18.6%

efficiency can be achieved for L8-BO [76] based bulk heterojunction organic solar cells revealing the immense potential of small molecular non-fullerene acceptors to realize high efficiency organic solar cells.

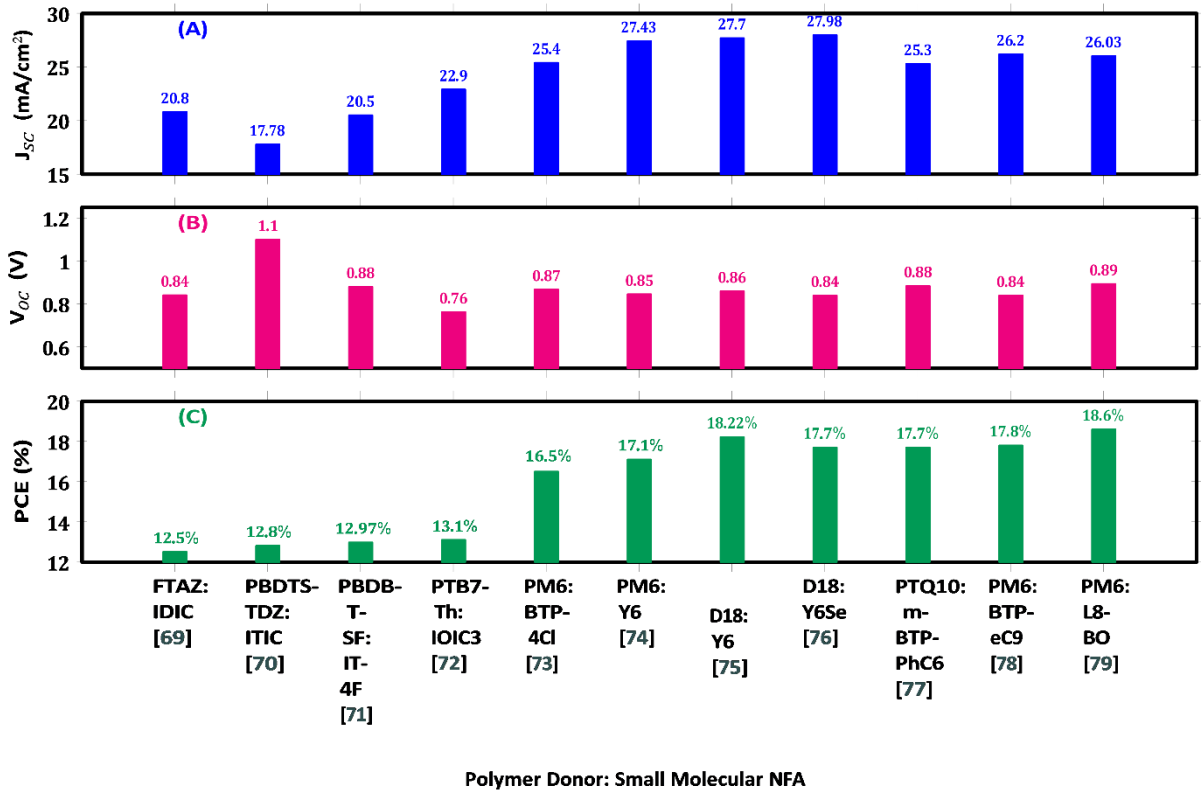

Figure 4.
(A) Short circuit current (B) open circuit voltage and (C) power conversion efficiency of some selected bulk heterojunction organic solar cells based on polymer doner/small molecule non-fullerene acceptors blends.
Source: Lin, et al. [66], Xu, et al. [67], Zhao, et al. [68], Zhu, et al. [69], Cui, et al. [70], Tran, et al. [71],Liu, et al. [72],Zhang, et al. [73], Chai, et al. [74], Cui, et al. [75] Song, et al. [76].

3.5.5. All Polymer Organic Solar Cells

All polymer organic solar cells [77] are polymer:polymer solar cells where conjugate polymers serve as p-type donors and rylene diimides-based polymer/small molecule non-fullerene acceptors act as n-type acceptors. These organic solar cells have the distinct advantages of electronic tunability, thermal, morphological, and photochemical stability as well as excellent mechanical properties [77]. To date, several Rylene diimides-based n-type polymers (PDI [78], NDI [79], BTI [80]) and small molecular non-fullerene acceptor (PYTM [81], PYF-T [82], PJ1-H [83], PYIT [84], PY2F-T [85], PZT [86]) have emerged as electron-deficient acceptor unit to construct the donor and acceptor interface. Plots in Figure 5(A-C) present the photovoltaic properties of device parameters of all- perovskite solar cells based on some selected rylene diimides based polymer acceptors and small molecular non-fullerene acceptors. The superiority of small molecule non-fullerene acceptor over rylene diimides is evident from the enhanced short circuit current, open circuit voltage and power conversion efficiency observed in these plots and reveals that small molecule non-fullerene acceptors are the better choice as n-type polymers owing to their excellent electronic and optical characteristics.

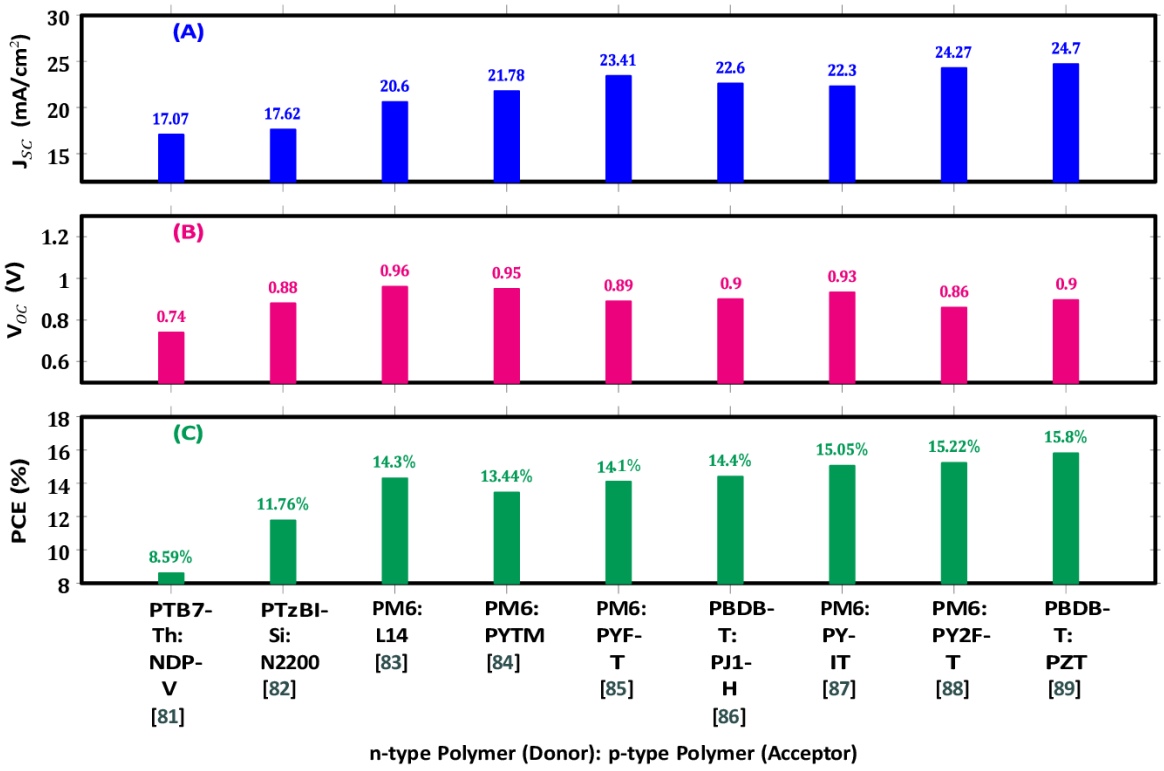

Figure 5.
(A) Short circuit current (B) open circuit voltage and (C) power conversion efficiency of some selected all-polymer organic solar cells.
Source: Guo, et al. [78], Zhu, et al. [79], Sun, et al. [80] Wang, et al. [81], Yu, et al. [82], Jia, et al. [83],Luo, et al. [84],Yu, et al. [85],Fu, et al. [86] and Genene, et al. [77] .

3.5.6. Ternary Organic Solar Cells

The absorption width exhibited by organic semiconductors is only 0.5 eV [87]; therefore, only a fraction of solar radiation can be absorbed by organic solar cells thereby limiting their power conversion efficiency. Enhanced absorption width while preserving the processing simplicity of bulk heterojunction organic solar cells can be achieved by employing a ternary heterojunction-based strategy where the heterojunction is formed by blending two donors (acceptors) with one acceptor (donor) resulting in a D1:D2: A (D: A1:A2) structure [87, 88]. The third component can tune the frontier HOMO-LUMO levels by adjusting its homogeneous phase formation with other donor and acceptor materials and modulate the electronic properties of the photoactive layer through film-morphology improvement [87].

The charge transfer mechanism in ternary organic solar cells is more intricate than its binary counterpart and depends on the third component's weight ratio, energy levels, and placement as well as the bandgap of all three materials in the blend. Four fundamental charge transfer mechanisms [87] (Figure 6) are identified: (i) charge transfer (ii) energy transfer (iii) parallel linkage and (iv) alloy model.

To achieve high PCE, the recent TOSCs employ narrow-bandgap (NBG) doner materials and NFAs. Figures 7(A-C) and Figures 8(A-C) present the performance metrics of D1:D2:A and D:A1:A2 structure-based TOSCs respectively.

D1: D2:A Structured TOSC: PTB7-Th: PffBT4T-2OD: PC71BM [89] and PTB7-Th: DIBC: PC71BM [90] are based on FDAs (PC71BM) with D1:D2:A structure and hence, show a low PCE of 10.72% and 12.17% respectively, as seen in Figure 7(C). Use of NFAs i.e. SFBRCN [91], IT-M [92] and IEICO-4F [93] materials increase the PCE further (→ 14%). NBG donor materials i.e. PBDT-ST [94] and PM6 [95-97] along with NFAs boost the efficiency to 16-17% and register a PCE of 17.53% for PM6: S3: Y6 [97]-based TOSCs.

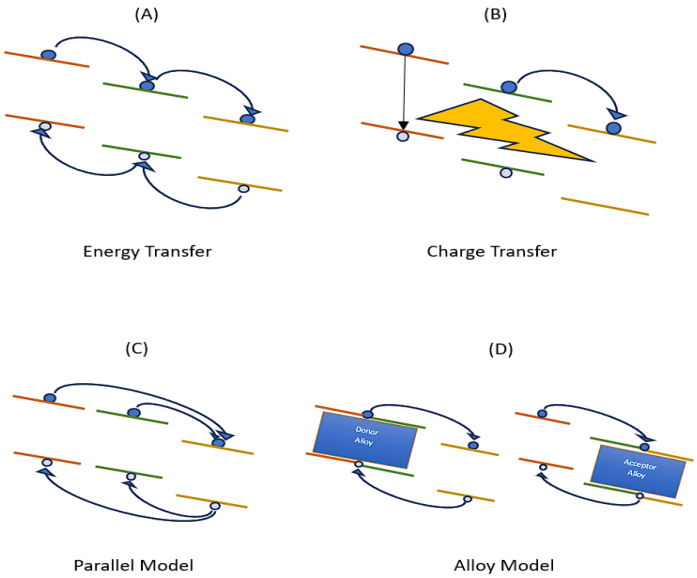

Figure 6.
Four fundamental charge transfer mechanisms in ternary OSCs.

D: A1: A2 Structured TOSC: For this structure, as seen in Figure 8(C), both fullerene derivative-based acceptors i.e. PC71BM [98, 99] and PC61BM [100] and NFAs i.e. MeIC [101], BTP-M [102], BTP-F [103], Y6 [104, 105] and L8-BO-F [106] show a significant increase in PCE ranging from 13.63% to 18.69%, which is also attributed to the use of NBG polymers (BTR, PM6 and D18-Cl). The highest PCE obtained for D:A1:A2 structured D18-Cl: N3: PC61BM-based TOSC is 18.69% [100].

3.6. Progress in PSCs Toward High PCE

Since the charge carrier generation, separation, and transport are the focal points of perovskite solar cells [110], judicious selection and preparation of electron transport layer (ETL), hole transport layer (HTL), perovskite layer, and electrodes increasingly attract the researchers' attention to increase efficiency with a reduction in cost.

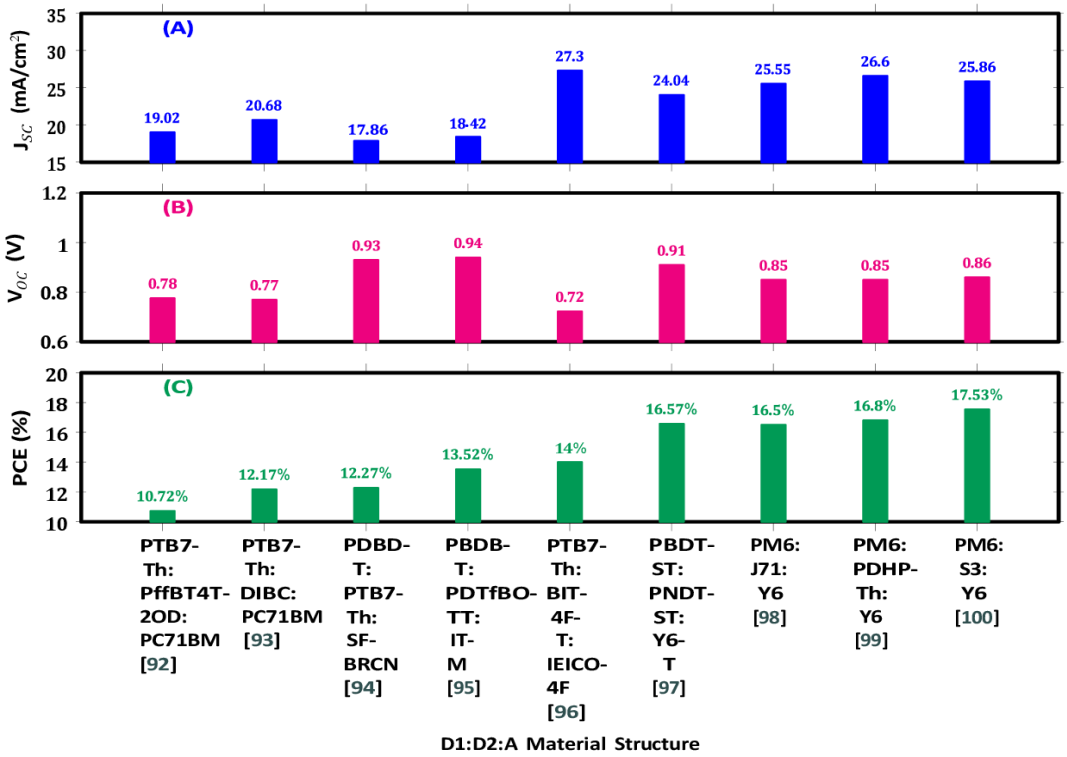

Figure 7.
(A) Short circuit current (B) open circuit voltage and (C) power conversion efficiency of some selected D1:D2:A structured ternary organic solar cells.
Source: Zhao, et al. [89], Du, et al. [90] ,Xu, et al. [91], Nian, et al. [92],Song, et al. [93], Xu, et al. [94], [95-97], Xie, et al. [95],Han, et al. [96],An, et al. [97].

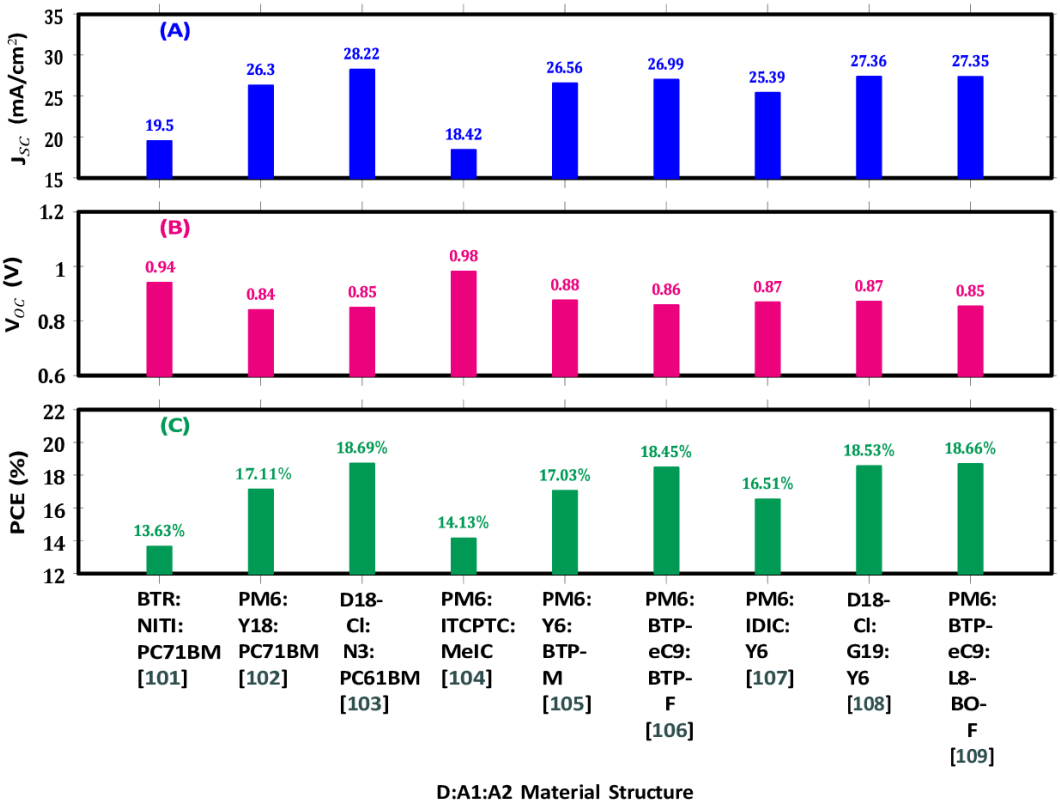

Figure 8.
(A) Short circuit current (B) open circuit voltage and (C) power conversion efficiency of some selected D:A1:A2 structured ternary organic solar cells.
Source: Zhou, et al. [98],Zhu, et al. [99], Jin, et al. [100], Liu, et al. [101], Zhan, et al. [102] , Li, et al. [103] ,Li, et al. [104],Chen, et al. [105], Cai, et al. [106].

3.6.1. Doped Electron Transport Layer

In perovskite solar cells, the electron transport layer enhances electron transport and blocks the hole transport to electrodes, for which an appropriate matching of the electronic energy levels of electron transport layer and the perovskites is required [107]. Indeed, it was noted that the perovskite material, slightly lowered conduction band, and much-lowered valence band of electron transport layer can ensure both efficient electron transport and effective hole blocking [108]. Oxides, namely, TiO_2, SnO_2 and ZnO are commonly used as electron transport layer for perovskite solar cells owing to their excellent electronic and optical properties as well as low-cost preparation. The ability of both dense and mesoporous layer formation makes TiO_2 attractive in mesoscopic perovskite solar cells [107]. Various doping materials are commonly used with all these electron transport layer materials to achieve higher efficiency of perovskite solar cells. For example, Mg [109], Ce [110], Li [111] Zn [112], Zr [113] are doped with TiO_2, Cl [114], Zr/F [115], Ta [116] are with SnO_2 and Mg [117], PbS [118]are with ZnO. Figures 9(A-C) plot the effects of these doped electron transport layer on short circuit current, open circuit voltage and power conversion efficiency of some selected perovskite solar cells based on FTO(ITO)/doped ETL/$MAPbI_3$/Spiro-OMeTAD/Au(Ag) device architecture. The highest efficiency reached (Figure 9(C)) 18.8%, 20.8% and 20.53% for perovskite solar cells based on electron transport layer with Zr-doped TiO_2 [113], Ta-doped SnO_2 [116], Zr/F [115], and PbS-doped ZnO [118], respectively.

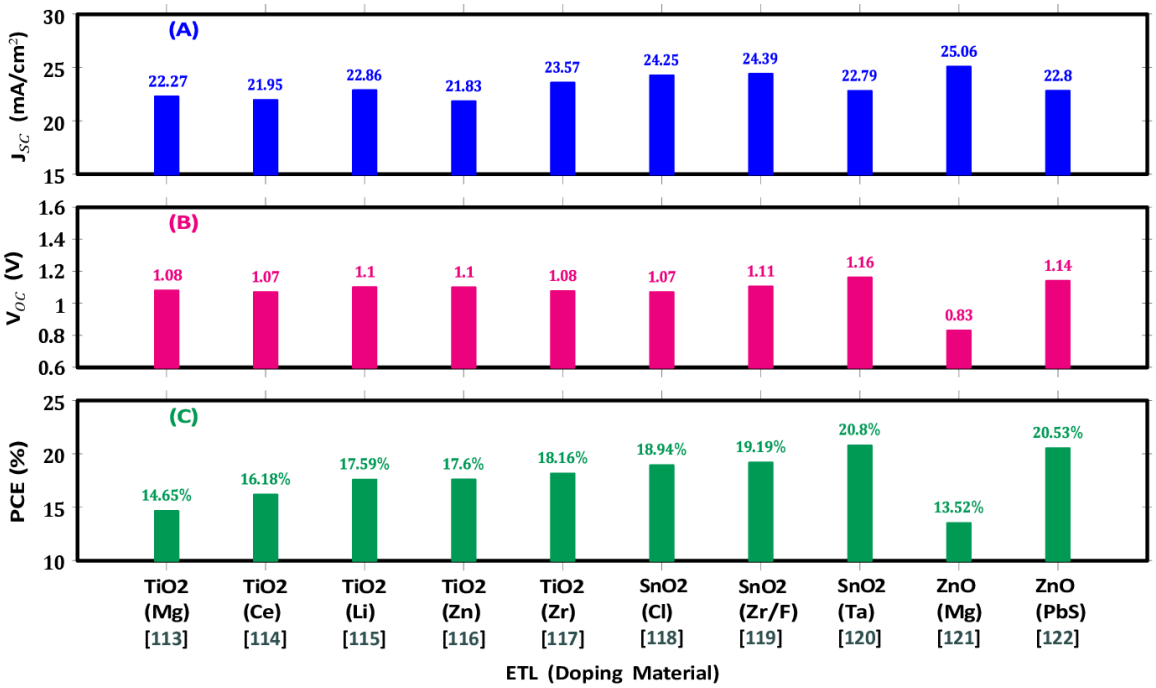

Figure 9.
Effects of different doped electron transport layer on (A) short circuit current (B) open circuit voltage and (C) power conversion efficiency of some selected perovskite solar cells.
Source: Arshad, et al. [109], Xu, et al. [110],Peter Amalathas, et al. [111], Liu, et al. [112], Sandhu, et al. [113] , Wu, et al. [114], Zr/F Tian, et al. [115], Liu, et al. [116], Arshad, et al. [117] and Pang, et al. [118].

3.6.2. Hole Transport Layer (HTL)

The hole transport layer performs the function of efficient hole extraction and electron blocking to avoid the interface compounding effectively [107] thereby playing vital role to achieving high efficiency of solar cells. The offset energy between the valence band energy levels of the hole transport layer and the perovskite drives the hole transport thereby increasing short circuit current; however, too large offset energy leads the increase (decrease) of V_{loss} (V_{OC}) [107]. The most common hole transport layers used include Spiro-OMeTAD, PEDOT: PSS and NiO.

Spiro-OMeTAD is a small-molecule organic semiconductor with excellent hole transport properties [107]. Although this hole transport layer is inherently unstable, various additive materials can be used to improve its stability. For example, 2D graphitic nitrogen-rich porous carbon can decrease the structural defects [119], Co(III)-grafted CN nanosheets ($CoCN_2$) can reduce the interface recombination [120] and Sb_2S_3 can increase the chemical stability [121]. SnS nanoparticles [122] and $PbSO_4(PbO)_4$ quantum dots [123] are also reported as useful additives to improve the stability of Spiro-OMeTAD. The device performance metrics plotted in Figures 10(A-C) reveal that Spiro-OMeTAD HTL-based perovskite solar cells have efficiency more than 18% and reached an efficiency of 23.01% for the PSC reported in Ref. [120].

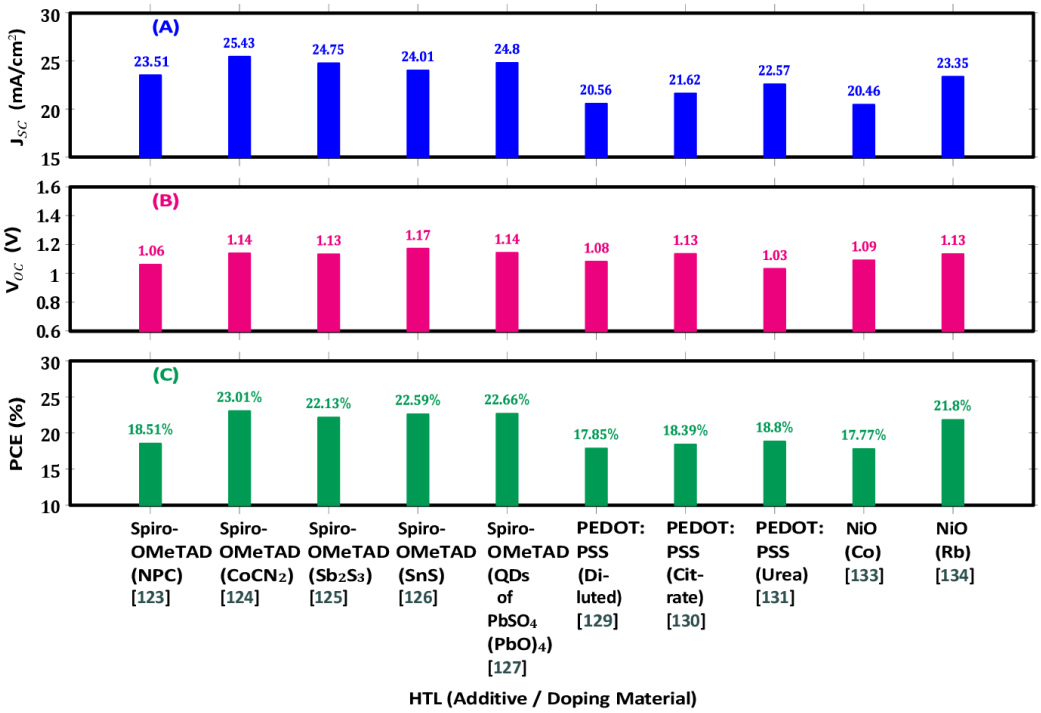

Figure 10.
Effects of different hole transport layer with additives/doping material on (A) short circuit current (B) open circuit voltage and (C) power conversion efficiency of some selected perovskite solar cells.
Source: Zhou, et al. [119], Cao, et al. [120], Du, et al. [121], Zheng, et al. [122], Zheng, et al. [123], Han, et al. [124], Yang, et al. [125], Elbohy, et al. [126], Hu, et al. [127], Xu, et al. [128], Lee, et al. [129] and Chen, et al. [130].

PEDOT:PSS is a low-temperature processable polymer with higher optical transparency, is commonly used as hole transport layer in inverted solar cells [107]. The limitations of this hole transport layer include low work function, low conductivity, and polarity mismatch with perovskite materials [124]. Diluted PEDOT: PSS can improve its work function [125], doping with sodium citrate can improve its functionality [127], and urea as an additive can adjust its work function and conductivity [126]- all of which lead to the efficiency of the perovskite solar cells based on PEDOT:PSS to surpass 17%. The highest efficiency of 18.8% was achieved with urea additives [126].

Low temperature processability and better stability than organic ones lead to the use of NiO as an inorganic hole transport layer in inverted perovskite solar cells. However, NiO suffers from the problems of band alignment mismatch and low conductivity [128]. Cobalt (Co) doping reduces the band alignment problem to reduce V_{loss} and hence, increases the efficiency to 17.77% [129]. Rubidium (Rb) doping increases conductivity and improves the band alignment thereby increasing the efficiency even higher (21.8%) [130].

3.6.3. Perovskite Layer

The improved stability with higher efficiency is a serious concern for perovskite solar cells and is limited by the perovskite film quality (surface roughness, grain size, and defects) [107]. Spin coating, spray coating, screen printing, vapor deposition, electrodeposition are some preparation processes reported [107]to prepare high-quality perovskite films. Except for the vapor deposition method, all are suitable for mass production. Spin coating method is environment-friendly; vapor deposition, suitable for small lab scale, needs to transform into a mass-level production scale and others need improvement in efficiency and repeatability [107]. The highest efficiency is 20.52% for screen printing [131]19.60% for inkjet printing [132], 23.56% for spin coating [133], 20.80% for blade coating [134], and 18.50% for vapor deposition method [135], respectively.

3.6.4. Electrodes

The electrode materials for perovskite solar cells should have characteristics of matched work function, lower electrical resistivity, stability, and higher performance/price ratio [107]. Therefore, research attempts are continuously carried out to explore new electrode materials with these traits instead of conventional noble metal electrodes (gold and silver). To date, carbon materials such as carbon nanotube [136], mesoporous carbon [137], carbon nanofiber [138], graphite [139], and graphene [140] are reported as ideal candidates with these characteristics.

3.7. Stability Issues of OSCs and PSCs

The stability in organic solar cells and perovskite solar cells is degraded by several mechanisms which include inherent, light, thermal, air, and mechanical instability, etc. Inherent instability is due to morphology change and carrier diffusion into the active layer [19], light instability is due to photophysical and photochemical degradation under illuminated conditions [141, 142], thermal instability is due to high operating temperature with continuous heating [141, 143] and air instability is due to diffusion of ambient oxygen and moisture water into the device [19, 141]. Mechanical

instability owing to the unavoidable mechanical stress occurs during device fabrication, installation, and transportation [144] as well as weather conditions (rain, wind etc.) [145]. Burn-in degradation degrades the initial performance degradation abruptly due to morphology changes in the active layer [146, 147] and contributes significantly to the instability of these solar cells.

3.7.1. Stability in Organic Solar Cells

The stability issues of organic solar cells require more research focus to apprehend the underlying mechanisms of device instability due to air, moisture, operating temperature, illumination, and mechanical stress. Improvement of photo/air stability can be accomplished by increasing the polymer crystallinity, for which cleavable sidechains and photo/air-stable units can be employed with donor type polymers. However, the increased crystallinity of polymers reduces the mechanical stability. Therefore, a balance in polymer crystallinity must be made for the simultaneous achievement of photo/air and mechanical stability.

Reduced crystallinity of non-fullerene acceptors enhances air and thermal stability. A well-designed stable donor and acceptor interface can improve both thermal and mechanical stability. Improvement of the photoactive layer/electrode interface and reduction of remaining solvents in the photoactive layer also enhance thermal stability.

Air stability can be enhanced by choosing electrode materials with low permeability of oxygen and moisture and, by selecting charge transport layers with inoxidizability. Highly flexible encapsulation materials can significantly improve mechanical stability.

3.7.2. Stability in Perovskite Solar Cells

The ABX_3 perovskite structure consists of a $[BX_6]^{4-}$ octahedra formed with sixfold coordinated B^{2+} cations surrounded by X sites where the cavity formed by the corner shared octahedra is occupied by A sites [17]. To make this structure stable, an appropriate combination of anions and cations must be chosen. Two empirical parameters the geometrical tolerance factor (t) and the octahedral factor (μ) are used to indicate this appropriate combination, which can be defined as [17]-

$$t = \frac{R_a + R_x}{\sqrt{2}(R_b + R_x)} \quad (6)$$

$$\mu = \frac{R_b}{R_x} \quad (7)$$

where R_a, R_b, and R_x denote the ionic radii of the A, B, and X sites, respectively. 't' assesses the fit of the A cation in the corner sharing octahedra, and μ estimates the fit of the B cation in the X_6 octahedron. Values of μ = 0.442-0.895 (empirically determined) can form a perovskite structure [17]. On the other hand, for the stability of a perovskite structure, values of t should be carefully chosen. For stable cubic structure, t=0.9-1; for stable, distorted orthorhombic/tetragonal structure, t=0.8-0.9 [17]. Perovskites with a stable, highly symmetric, cubic structure require t=0.813−1.107. formamidine (r_a=253 pm), being larger than methylammonium (r_a=217 pm) and caesium (r_a=167 pm), has slight structural distortions; however, formamidine has higher t value, and hence, is more stable than methylammonium and caesium [16]. Therefore, one effective strategy to ensure both stability and high efficiency is composition engineering. This engineering includes partial or full substitution of A- site cation and X-site halide anion with appropriate material and addition of some additive materials- all of which not only enhance the efficiency by improving the optoelectronic properties but also ensure thermal stability. The rational choice of charge transport layer to maintain appropriate band alignment between them and the perovskites is another strategy to improve both efficiency and thermal stability. To ensure the intrinsic stability of the perovskite films several defect passivation techniques such as film synthesis and post-treatment conditions, interlayer engineering, grain passivation, are employed to reduce lattice imperfections. Instability due to moisture and oxygen can be minimized by proper encapsulation strategies [16].

The presence of lead (Pb) in Pb-based high-efficiency perovskite solar cells also issues a higher level of concern over material toxicity as compared with organic solar cells. Among various elements (Sb, Sn, Bi, Cu, and Ge), Sn (tin) is the best alternative to Pb in Pb-free perovskite solar cells because of its Pb-like electronic configuration and hence, Pb-ion in the B site can be directly replaced with the Sn ions without changing the phase significantly. However, tin-based perovskite solar cells attain much lower efficiency (10-12%) [148, 149] and suffer from less stability as compared to Pb-based organic solar cells.

4. Conclusion

The ongoing development of organic and perovskite solar cells is testament in the possibilities of renewable energy generation, and emphasis the need on how fabrication issues can be addressed for other approaches. Perovskite solar cell advances demonstrate how efficient gains can be extracted from solar energy. Perovskites have a combination of material properties and structural designs that make them ripe for the next generation of renewable energy technologies. Though the efficiency of perovskite solar cells has exceeded 23%, their stability is the largest problem to be solved. By comparison, organic solar cells suffer from both efficiency and stability constraints. Therefore, although to date there have been several advantages of organic solar cells and perovskite solar cells over traditional silicon-based solar cells, the successful application of organic solar cells and perovskite solar cells has not been fully achieved. Organic solar cells suffer from limited performance owing to a stronger electron-phonon coupling, higher nonradiative recombination rates, and huge

energy loss in polaron formation. Therefore, the key barriers for organic solar cells with both high efficiency and good stability need to be overcome to regulate nanomorphology, reduce trap state density and trap state distribution, and improve effective carrier mobility. By contrast, along with perovskite solar cells, issues of prime importance are reduction of recombination losses being accrued from charge trapping at grain boundaries and those at the interfaces of the active layer with the charge extraction layers, themselves as well as in the composition of the charge extraction layers.

References

[1] M. Kouihi, S. Bikndaren, M. Moutchou, A. A. ElMahjoub, and R. Majdoul, "Comprehensive review of classical and ai-driven energy management strategies for hybrid renewable energy systems," *E-Prime - Advances in Electrical Engineering, Electronics and Energy*, vol. 13, p. 101085, 2025. https://doi.org/10.1016/j.prime.2025.101085

[2] G. A. Nowsherwan *et al.*, "Numerical optimization and performance evaluation of ZnPC:PC70BM based dye-sensitized solar cell," *Scientific Reports*, vol. 13, no. 1, p. 10431, 2023. https://doi.org/10.1038/s41598-023-37486-2

[3] K. Nguyen *et al.*, "Optimizing energy yield of monolithic perovskite/silicon tandem solar cells in real-world Conditions: The impact of luminescent coupling," *Solar Energy Materials and Solar Cells*, vol. 290, p. 113730, 2025. https://doi.org/10.1016/j.solmat.2025.113730

[4] E. T. Ymer, H. G. Lemu, and M. A. Tolcha, "Identification of the key material degradation mechanisms affecting silicon solar cells: Systematic literature review," *Results in Engineering*, vol. 27, p. 106113, 2025. https://doi.org/10.1016/j.rineng.2025.106113

[5] M. Wang, J. He, L. Zheng, T. Alkhalifah, and R. Marzouki, "Optimizing energy capacity, and vibration control performance of multi-layer smart silicon solar cells using mathematical simulation and deep neural networks," *Aerospace Science and Technology*, vol. 159, p. 109983, 2025. https://doi.org/10.1016/j.ast.2025.109983

[6] A. Sri, Manju Venkatachalam, Chitra Devi, R. Rathanasamy, and S. Sivaraj, "Utilisation of SiO2/TiO2/Al2O3 mechanical blends for enhancing the photovoltaic efficiency in polycrystalline silicon solar cells," *Surfaces and Interfaces*, vol. 65, p. 106466, 2025. https://doi.org/10.1016/j.surfin.2025.106466

[7] J. Wu *et al.*, "A comparison of charge carrier dynamics in organic and perovskite solar cells," *Advanced Materials*, vol. 34, no. 2, p. 2101833, 2022. https://doi.org/10.1002/adma.202101833

[8] P. Roy, A. Ghosh, F. Barclay, A. Khare, and E. Cuce, "Perovskite solar cells: A review of the recent advances," *Coatings*, vol. 12, no. 8, p. 1089, 2022. https://doi.org/10.3390/coatings12081089

[9] M. A. Saeed *et al.*, "Indoor organic photovoltaics: Optimal cell design principles with synergistic parasitic resistance and optical modulation effect," *Advanced Energy Materials*, vol. 11, no. 27, p. 2003103, 2021. https://doi.org/10.1002/aenm.202003103

[10] S. Ghosh and R. Yadav, "Future of photovoltaic technologies: A comprehensive review," *Sustainable Energy Technologies and Assessments*, vol. 47, p. 101410, 2021. https://doi.org/10.1016/j.seta.2021.101410

[11] M. Tawalbeh, A. Al-Othman, F. Kafiah, E. Abdelsalam, F. Almomani, and M. Alkasrawi, "Environmental impacts of solar photovoltaic systems: A critical review of recent progress and future outlook," *Science of The Total Environment*, vol. 759, p. 143528, 2021. https://doi.org/10.1016/j.scitotenv.2020.143528

[12] A. M. Bagher, M. M. A. Vahid, and M. Mohsen, "Types of solar cells and application," *American Journal of optics and Photonics*, vol. 3, no. 5, pp. 94-113, 2015.

[13] A. S. R. Bati, Y. L. Zhong, P. L. Burn, M. K. Nazeeruddin, P. E. Shaw, and M. Batmunkh, "Next-generation applications for integrated perovskite solar cells," *Communications Materials*, vol. 4, no. 1, p. 2, 2023. https://doi.org/10.1038/s43246-022-00325-4

[14] Y. Ma, Z. Lu, X. Su, G. Zou, and Q. Zhao, "Recent progress toward commercialization of flexible perovskite solar cells: from materials and structures to mechanical stabilities," *Advanced Energy and Sustainability Research*, vol. 4, no. 1, p. 2200133, 2023. https://doi.org/10.1002/aesr.202200133

[15] M. A. Green, "Self-consistent optical parameters of intrinsic silicon at 300K including temperature coefficients," *Solar Energy Materials and Solar Cells*, vol. 92, no. 11, pp. 1305-1310, 2008. https://doi.org/10.1016/j.solmat.2008.06.009

[16] J. Chen *et al.*, "Recent progress in stabilizing hybrid perovskites for solar cell applications," *Journal of Power Sources*, vol. 355, pp. 98-133, 2017. https://doi.org/10.1016/j.jpowsour.2017.04.025

[17] M. Pitaro, E. K. Tekelenburg, S. Shao, and M. A. Loi, "Tin halide perovskites: From fundamental properties to solar cells," *Advanced Materials*, vol. 34, no. 1, p. 2105844, 2022. https://doi.org/10.1002/adma.202105844

[18] N. J. Jeon *et al.*, "A fluorene-terminated hole-transporting material for highly efficient and stable perovskite solar cells," *Nature Energy*, vol. 3, no. 8, pp. 682-689, 2018. https://doi.org/10.1038/s41560-018-0200-6

[19] L. Duan and A. Uddin, "Progress in stability of organic solar cells," *Advanced Science*, vol. 7, no. 1, p. 1903259, 2020. https://doi.org/10.1002/advs.201903259

[20] C. W. Tang, "Two-layer organic photovoltaic cell," *Applied Physics Letters*, vol. 48, no. 2, pp. 183-185, 1986. https://doi.org/10.1063/1.96937

[21] S. Holliday *et al.*, "High-efficiency and air-stable P3HT-based polymer solar cells with a new non-fullerene acceptor," *Nature Communications*, vol. 7, no. 1, p. 11585, 2016. https://doi.org/10.1038/ncomms11585

[22] J. Zhang, H. S. Tan, X. Guo, A. Facchetti, and H. Yan, "Material insights and challenges for non-fullerene organic solar cells based on small molecular acceptors," *Nature Energy*, vol. 3, no. 9, pp. 720-731, 2018. https://doi.org/10.1038/s41560-018-0181-5

[23] P. W. Blom, V. D. Mihailetchi, L. J. A. Koster, and D. E. Markov, "Device physics of polymer: Fullerene bulk heterojunction solar cells," *Advanced Materials*, vol. 19, no. 12, pp. 1551-1566, 2007. https://doi.org/10.1002/adma.200601093

[24] D. E. Markov, E. Amsterdam, P. W. M. Blom, A. B. Sieval, and J. C. Hummelen, "Accurate measurement of the exciton diffusion length in a conjugated polymer using a heterostructure with a side-chain cross-linked fullerene layer," *The Journal of Physical Chemistry A*, vol. 109, no. 24, pp. 5266-5274, 2005. https://doi.org/10.1021/jp0509663

[25] C. M. Wolff, P. Caprioglio, M. Stolterfoht, and D. Neher, "Nonradiative recombination in perovskite solar cells: The role of interfaces," *Advanced Materials*, vol. 31, no. 52, p. 1902762, 2019. https://doi.org/10.1002/adma.201902762

[26] A. D. Wright *et al.*, "Electron–phonon coupling in hybrid lead halide perovskites," *Nature Communications*, vol. 7, no. 1, p. 11755, 2016. https://doi.org/10.1038/ncomms11755
[27] Z. Liu *et al.*, "Open-circuit voltages exceeding 1.26 V in planar methylammonium lead iodide perovskite solar cells," *ACS Energy Letters*, vol. 4, no. 1, pp. 110-117, 2018. https://doi.org/10.1021/acsenergylett.8b01906
[28] S. D. Dimitrov *et al.*, "Spectroscopic investigation of the effect of microstructure and energetic offset on the nature of interfacial charge transfer states in polymer: Fullerene blends," *Journal of the American Chemical Society*, vol. 141, no. 11, pp. 4634-4643, 2019. https://doi.org/10.1021/jacs.8b11484
[29] J. Kim *et al.*, "Excitation density dependent photoluminescence quenching and charge transfer efficiencies in hybrid perovskite/organic semiconductor bilayers," *Advanced Energy Materials*, vol. 8, no. 35, p. 1802474, 2018. https://doi.org/10.1002/aenm.201802474
[30] Y. Zhu, F. Zhao, W. Wang, Y. Li, S. Zhang, and Y. Lin, "Exciton binding energy of non-fullerene electron acceptors," *Advanced Energy and Sustainability Research*, vol. 3, no. 4, p. 2100184, 2022. https://doi.org/10.1002/aesr.202100184
[31] X. Xu, G. Zhang, Y. Li, and Q. Peng, "The recent progress of wide bandgap donor polymers towards non-fullerene organic solar cells," *Chinese Chemical Letters*, vol. 30, no. 4, pp. 809-825, 2019. https://doi.org/10.1016/j.cclet.2019.02.030
[32] X.-P. Xu, Y. Li, M.-M. Luo, and Q. Peng, "Recent progress towards fluorinated copolymers for efficient photovoltaic applications," *Chinese Chemical Letters*, vol. 27, no. 8, pp. 1241-1249, 2016. https://doi.org/10.1016/j.cclet.2016.05.006
[33] V. A. Trukhanov, V. V. Bruevich, and D. Y. Paraschuk, "Fill factor in organic solar cells can exceed the Shockley-Queisser limit," *Scientific Reports*, vol. 5, no. 1, p. 11478, 2015. https://doi.org/10.1038/srep11478
[34] H. Uratani and K. Yamashita, "Charge carrier trapping at surface defects of perovskite solar cell absorbers: A first-principles study," *The Journal of Physical Chemistry Letters*, vol. 8, no. 4, pp. 742-746, 2017. https://doi.org/10.1021/acs.jpclett.7b00055
[35] M. P. Nikiforov *et al.*, "Detection and role of trace impurities in high-performance organic solar cells," *Energy & Environmental Science*, vol. 6, no. 5, pp. 1513-1520, 2013.
[36] T. Du *et al.*, "Probing and controlling intragrain crystallinity for improved low temperature–processed perovskite solar cells," *Advanced Functional Materials*, vol. 28, no. 51, p. 1803943, 2018. https://doi.org/10.1002/adfm.201803943
[37] C. M. Proctor, M. Kuik, and T.-Q. Nguyen, "Charge carrier recombination in organic solar cells," *Progress in Polymer Science*, vol. 38, no. 12, pp. 1941-1960, 2013. https://doi.org/10.1016/j.progpolymsci.2013.08.008
[38] H. K. H. Lee *et al.*, "Organic photovoltaic cells–promising indoor light harvesters for self-sustainable electronics," *Journal of Materials Chemistry A*, vol. 6, no. 14, pp. 5618-5626, 2018.
[39] S.-H. Turren-Cruz *et al.*, "Enhanced charge carrier mobility and lifetime suppress hysteresis and improve efficiency in planar perovskite solar cells," *Energy & Environmental Science*, vol. 11, no. 1, pp. 78-86, 2018.
[40] G. F. A. Dibb *et al.*, "Influence of doping on charge carrier collection in normal and inverted geometry polymer:Fullerene solar cells," *Scientific Reports*, vol. 3, no. 1, p. 3335, 2013. https://doi.org/10.1038/srep03335
[41] T. Kirchartz, T. Agostinelli, M. Campoy-Quiles, W. Gong, and J. Nelson, "Understanding the thickness-dependent performance of organic bulk heterojunction solar cells: The influence of mobility, lifetime, and space charge," *The journal of physical chemistry letters*, vol. 3, no. 23, pp. 3470-3475, 2012. https://doi.org/10.1021/jz301639y
[42] J. Wu *et al.*, "Tail state limited photocurrent collection of thick photoactive layers in organic solar cells," *Nature Communications*, vol. 10, no. 1, p. 5159, 2019. https://doi.org/10.1038/s41467-019-12951-7
[43] S. Chen *et al.*, "Ultrafast Channel II process induced by a 3-D texture with enhanced acceptor order ranges for high-performance non-fullerene polymer solar cells," *Energy & Environmental Science*, vol. 11, no. 9, pp. 2569-2580, 2018.
[44] N. S. Sariciftci, L. Smilowitz, A. J. Heeger, and F. Wudl, "Photoinduced electron transfer from a conducting polymer to buckminsterfullerene," *Science*, vol. 258, no. 5087, pp. 1474-1476, 1992. https://doi.org/10.1016/j.jphotochem.2025.116641
[45] G. Li *et al.*, "High-efficiency solution processable polymer photovoltaic cells by self-organization of polymer blends," *Nature Materials*, vol. 4, no. 11, pp. 864-868, 2005. https://doi.org/10.1038/nmat1500
[46] P. A. Troshin *et al.*, "Material solubility-photovoltaic performance relationship in the design of novel fullerene derivatives for bulk heterojunction solar cells," *Advanced Functional Materials*, vol. 19, no. 5, pp. 779-788, 2009. https://doi.org/10.1002/adfm.200801189
[47] H. U. Kim *et al.*, "Naphthalene-, anthracene-, and pyrene-substituted fullerene derivatives as electron acceptors in polymer-based solar cells," *ACS Applied Materials & Interfaces*, vol. 6, no. 23, pp. 20776-20785, 2014. https://doi.org/10.1021/am504939c
[48] M. Lenes, G. J. A. Wetzelaer, F. B. Kooistra, S. C. Veenstra, J. C. Hummelen, and P. W. Blom, "Fullerene bisadducts for enhanced open-circuit voltages and efficiencies in polymer solar cells," *Advanced Materials*, vol. 20, no. 11, pp. 2116-2119, 2008. https://doi.org/10.1002/adma.200702438
[49] J. A. Mikroyannidis, A. N. Kabanakis, S. Sharma, and G. D. Sharma, "A simple and effective modification of PCBM for use as an electron acceptor in efficient bulk heterojunction solar cells," *Advanced Functional Materials*, vol. 21, no. 4, pp. 746-755, 2011. https://doi.org/10.1002/adfm.201001807
[50] G. Zhao *et al.*, "Effect of carbon chain length in the substituent of PCBM-like molecules on their photovoltaic properties," *Advanced Functional Materials*, vol. 20, no. 9, pp. 1480-1487, 2010. https://doi.org/10.1002/adfm.200902447
[51] Y. He, H.-Y. Chen, J. Hou, and Y. Li, "Indene− C60 bisadduct: A new acceptor for high-performance polymer solar cells," *Journal of the American Chemical Society*, vol. 132, no. 4, pp. 1377-1382, 2010.
[52] G. Zhao, Y. He, and Y. Li, "6.5% efficiency of polymer solar cells based on poly (3-hexylthiophene) and indene-C60 bisadduct by device optimization," *Advanced Materials*, vol. 22, no. 39, pp. 4355-4358, 2010. https://doi.org/10.1002/adma.201001339
[53] Y. He, G. Zhao, B. Peng, and Y. Li, "High-yield synthesis and electrochemical and photovoltaic properties of indene-C70 bisadduct," *Advanced Functional Materials*, vol. 20, no. 19, pp. 3383-3389, 2010. https://doi.org/10.1002/adfm.201001122
[54] J. Peet *et al.*, "Efficiency enhancement in low-bandgap polymer solar cells by processing with alkane dithiols," *Nature Materials*, vol. 6, no. 7, pp. 497-500, 2007. https://doi.org/10.1038/nmat1928
[55] Y. Liang *et al.*, "Development of new semiconducting polymers for high performance solar cells," *Journal of the American Chemical Society*, vol. 131, no. 1, pp. 56-57, 2009. https://doi.org/10.1021/ja808373p
[56] Y. Liang *et al.*, "For the bright future-bulk heterojunction polymer solar cells with power conversion efficiency of 7.4%," *Advanced Materials*, vol. 22, no. 20, p. E135, 2010.

[57] Z. He, C. Zhong, S. Su, M. Xu, H. Wu, and Y. Cao, "Enhanced power-conversion efficiency in polymer solar cells using an inverted device structure," *Nature Photonics*, vol. 6, no. 9, pp. 591-595, 2012. https://doi.org/10.1038/nphoton.2012.190

[58] S.-H. Liao, H.-J. Jhuo, Y.-S. Cheng, and S.-A. Chen, "Fullerene derivative-doped zinc oxide nanofilm as the cathode of inverted polymer solar cells with low-bandgap polymer (PTB7-Th) for high performance," *Advanced Materials*, vol. 25, no. 34, pp. 4766-4771, 2013.

[59] J. D. Chen *et al.*, "Single-junction polymer solar cells exceeding 10% power conversion efficiency," *Advanced Materials*, vol. 27, no. 6, pp. 1035-1041, 2015.

[60] H.-Y. Chen *et al.*, "Polymer solar cells with enhanced open-circuit voltage and efficiency," *Nature Photonics*, vol. 3, no. 11, pp. 649-653, 2009. https://doi.org/10.1038/nphoton.2009.192

[61] Y. Liu *et al.*, "Aggregation and morphology control enables multiple cases of high-efficiency polymer solar cells," *Nature Communications*, vol. 5, no. 1, p. 5293, 2014. https://doi.org/10.1038/ncomms6293

[62] J. Zhao *et al.*, "Efficient organic solar cells processed from hydrocarbon solvents," *Nature Energy*, vol. 1, no. 2, p. 15027, 2016. https://doi.org/10.1038/nenergy.2015.27

[63] Y. Liu *et al.*, "Recent progress in organic solar cells (Part II device engineering)," *Science China Chemistry*, vol. 65, no. 8, pp. 1457-1497, 2022. https://doi.org/10.1007/s11426-022-1256-8

[64] H. Fu, Z. Wang, and Y. Sun, "Polymer donors for high-performance non-fullerene organic solar cells," *Angewandte Chemie International Edition*, vol. 58, no. 14, pp. 4442-4453, 2019. https://doi.org/10.1002/anie.201806291

[65] G. Zhang *et al.*, "Nonfullerene acceptor molecules for bulk heterojunction organic solar cells," *Chemical reviews*, vol. 118, no. 7, pp. 3447-3507, 2018. https://doi.org/10.1021/acs.chemrev.7b00535

[66] Y. Lin *et al.*, "Balanced partnership between donor and acceptor components in nonfullerene organic solar cells with> 12% efficiency," *Advanced Materials*, vol. 30, no. 16, p. 1706363, 2018. https://doi.org/10.1002/adma.201706363

[67] X. Xu, T. Yu, Z. Bi, W. Ma, Y. Li, and Q. Peng, "Realizing over 13% efficiency in green-solvent-processed nonfullerene organic solar cells enabled by 1, 3, 4-thiadiazole-based wide-bandgap copolymers," *Advanced Materials*, vol. 30, no. 3, p. 1703973, 2018. https://doi.org/10.1002/adma.201703973

[68] W. Zhao *et al.*, "Molecular optimization enables over 13% efficiency in organic solar cells," *Journal of the American Chemical Society*, vol. 139, no. 21, pp. 7148-7151, 2017. https://doi.org/10.1021/jacs.7b02677

[69] J. Zhu *et al.*, "Alkoxy-induced near-infrared sensitive electron acceptor for high-performance organic solar cells," *Chemistry of Materials*, vol. 30, no. 12, pp. 4150-4156, 2018. https://doi.org/10.1021/acs.chemmater.8b01677

[70] Y. Cui *et al.*, "Over 16% efficiency organic photovoltaic cells enabled by a chlorinated acceptor with increased open-circuit voltages," *Nature Communications*, vol. 10, no. 1, p. 2515, 2019. https://doi.org/10.1038/s41467-019-10351-5

[71] H. N. Tran *et al.*, "17% non-fullerene organic solar cells with annealing-free aqueous MoOx," *Advanced Science*, vol. 7, no. 21, p. 2002395, 2020. https://doi.org/10.1002/advs.202002395

[72] Q. Liu *et al.*, "18% Efficiency organic solar cells," *Science Bulletin*, vol. 65, no. 4, pp. 272-275, 2020.

[73] Z. Zhang, Y. Li, G. Cai, Y. Zhang, X. Lu, and Y. Lin, "Selenium heterocyclic electron acceptor with small urbach energy for as-cast high-performance organic solar cells," *Journal of the American Chemical Society*, vol. 142, no. 44, pp. 18741-18745, 2020. https://doi.org/10.1021/jacs.0c08557

[74] G. Chai *et al.*, "Fine-tuning of side-chain orientations on nonfullerene acceptors enables organic solar cells with 17.7% efficiency," *Energy & Environmental Science*, vol. 14, no. 6, pp. 3469-3479, 2021.

[75] Y. Cui *et al.*, "Single-junction organic photovoltaic cells with approaching 18% efficiency," *Advanced Materials*, vol. 32, no. 19, p. 1908205, 2020. https://doi.org/10.1002/adma.201908205

[76] J. Song *et al.*, "High-efficiency organic solar cells with low voltage loss induced by solvent additive strategy," *Matter*, vol. 4, no. 7, pp. 2542-2552, 2021. https://doi.org/10.1016/j.matt.2021.06.010

[77] Z. Genene, W. Mammo, E. Wang, and M. R. Andersson, "Recent advances in n-type polymers for all-polymer solar cells," *Advanced Materials*, vol. 31, no. 22, p. 1807275, 2019. https://doi.org/10.1002/adma.201807275

[78] Y. Guo *et al.*, "Improved performance of all-polymer solar cells enabled by naphthodiperylenetetraimide-based polymer acceptor," *Advanced materials*, vol. 29, no. 26, p. 1700309, 2017. https://doi.org/10.1002/adma.201700309

[79] L. Zhu *et al.*, "Aggregation-induced multilength scaled morphology enabling 11.76% efficiency in all-polymer solar cells using printing fabrication," *Advanced Materials*, vol. 31, no. 41, p. 1902899, 2019. https://doi.org/10.1002/adma.201902899

[80] H. Sun *et al.*, "A narrow-bandgap n-type polymer with an acceptor–acceptor backbone enabling efficient all-polymer solar cells," *Advanced Materials*, vol. 32, no. 43, p. 2004183, 2020. https://doi.org/10.1002/adma.202004183

[81] W. Wang *et al.*, "Controlling molecular mass of low-band-gap polymer acceptors for high-performance all-polymer solar cells," *Joule*, vol. 4, no. 5, pp. 1070-1086, 2020. https://doi.org/10.1016/j.joule.2020.03.019

[82] H. Yu *et al.*, "Fluorinated end group enables high-performance all-polymer solar cells with near-infrared absorption and enhanced device efficiency over 14%," *Advanced Energy Materials*, vol. 11, no. 4, p. 2003171, 2021. https://doi.org/10.1002/aenm.202003171

[83] T. Jia *et al.*, "14.4% efficiency all-polymer solar cell with broad absorption and low energy loss enabled by a novel polymer acceptor," *Nano Energy*, vol. 72, p. 104718, 2020. https://doi.org/10.1016/j.nanoen.2020.104718

[84] Z. Luo *et al.*, "Precisely controlling the position of bromine on the end group enables well-regular polymer acceptors for all-polymer solar cells with efficiencies over 15%," *Advanced Materials*, vol. 32, no. 48, p. 2005942, 2020. https://doi.org/10.1002/adma.202005942

[85] H. Yu *et al.*, "A difluoro-monobromo end group enables high-performance polymer acceptor and efficient all-polymer solar cells processable with green solvent under ambient condition," *Advanced Functional Materials*, vol. 31, no. 25, p. 2100791, 2021. https://doi.org/10.1002/adfm.202100791

[86] H. Fu *et al.*, "High efficiency (15.8%) all-polymer solar cells enabled by a regioregular narrow bandgap polymer acceptor," *Journal of the American Chemical Society*, vol. 143, no. 7, pp. 2665-2670, 2021.

[87] P. Bi and X. Hao, "Versatile ternary approach for novel organic solar cells: A review," *Solar RRL*, vol. 3, no. 1, p. 1800263, 2019. https://doi.org/10.1002/solr.201800263

[88] Y. Li *et al.*, "Recent progress in organic solar cells: A review on materials from acceptor to donor," *Molecules*, vol. 27, no. 6, p. 1800, 2022. https://doi.org/10.3390/molecules27061800

[89] F. Zhao *et al.*, "Combining energy transfer and optimized morphology for highly efficient ternary polymer solar cells," *Advanced Energy Materials*, vol. 7, no. 13, p. 1602552, 2017. https://doi.org/10.1002/aenm.201602552

[90] X. Du *et al.*, "Hydrogen bond induced green solvent processed high performance ternary organic solar cells with good tolerance on film thickness and blend ratios," *Advanced Functional Materials*, vol. 29, no. 30, p. 1902078, 2019. https://doi.org/10.1002/adfm.201902078

[91] X. Xu *et al.*, "Highly efficient ternary-blend polymer solar cells enabled by a nonfullerene acceptor and two polymer donors with a broad composition tolerance," *Advanced Materials*, vol. 29, no. 46, p. 1704271, 2017. https://doi.org/10.1002/adma.201704271

[92] L. Nian *et al.*, "Ternary non-fullerene polymer solar cells with 13.51% efficiency and a record-high fill factor of 78.13%," *Energy & Environmental Science*, vol. 11, no. 12, pp. 3392-3399, 2018.

[93] X. Song *et al.*, "Dual sensitizer and processing-aid behavior of donor enables efficient ternary organic solar cells," *Joule*, vol. 3, no. 3, pp. 846-857, 2019. https://doi.org/10.1016/j.joule.2019.01.009

[94] X. Xu, K. Feng, Y. W. Lee, H. Y. Woo, G. Zhang, and Q. Peng, "Subtle polymer donor and molecular acceptor design enable efficient polymer solar cells with a very small energy loss," *Advanced Functional Materials*, vol. 30, no. 9, p. 1907570, 2020. https://doi.org/10.1002/adfm.201907570

[95] G. Xie, Z. Zhang, Z. Su, X. Zhang, and J. Zhang, "16.5% efficiency ternary organic photovoltaics with two polymer donors by optimizing molecular arrangement and phase separation," *Nano Energy*, vol. 69, p. 104447, 2020. https://doi.org/10.1016/j.nanoen.2020.104447

[96] J. Han, X. Wang, D. Huang, C. Yang, R. Yang, and X. Bao, "Employing asymmetrical thieno [3, 4-d] pyridazin-1 (2 H)-one Block enables efficient ternary polymer solar cells with improved light-harvesting and morphological properties," *Macromolecules*, vol. 53, no. 15, pp. 6619-6629, 2020.

[97] Q. An *et al.*, "Two compatible polymer donors contribute synergistically for ternary organic solar cells with 17.53% efficiency," *Energy & Environmental Science*, vol. 13, no. 12, pp. 5039-5047, 2020.

[98] Z. Zhou *et al.*, "High-efficiency small-molecule ternary solar cells with a hierarchical morphology enabled by synergizing fullerene and non-fullerene acceptors," *Nature Energy*, vol. 3, no. 11, pp. 952-959, 2018. https://doi.org/10.1038/s41560-018-0234-9

[99] C. Zhu *et al.*, "Tuning the electron-deficient core of a non-fullerene acceptor to achieve over 17% efficiency in a single-junction organic solar cell," *Energy & Environmental Science*, vol. 13, no. 8, pp. 2459-2466, 2020.

[100] K. Jin, Z. Xiao, and L. Ding, "18.69% PCE from organic solar cells," *J. Semicond*, vol. 42, no. 6, p. 060502, 2021.

[101] T. Liu *et al.*, "Use of two structurally similar small molecular acceptors enabling ternary organic solar cells with high efficiencies and fill factors," *Energy & Environmental Science*, vol. 11, no. 11, pp. 3275-3282, 2018.

[102] L. Zhan *et al.*, "Over 17% efficiency ternary organic solar cells enabled by two non-fullerene acceptors working in an alloy-like model," *Energy & Environmental Science*, vol. 13, no. 2, pp. 635-645, 2020.

[103] Y. Li *et al.*, "A facile strategy for third-component selection in non-fullerene acceptor-based ternary organic solar cells," *Energy & Environmental Science*, vol. 14, no. 9, pp. 5009-5016, 2021.

[104] K. Li *et al.*, "Ternary blended fullerene-free polymer solar cells with 16.5% efficiency enabled with a higher-LUMO-level acceptor to improve film morphology," *Advanced Energy Materials*, vol. 9, no. 33, p. 1901728, 2019. https://doi.org/10.1002/aenm.201901728

[105] Z. Chen *et al.*, "Small-molecular donor guest achieves rigid 18.5% and flexible 15.9% efficiency organic photovoltaic via fine-tuning microstructure morphology," *Joule*, vol. 5, no. 9, pp. 2395-2407, 2021. https://doi.org/10.1016/j.joule.2021.06.017

[106] Y. Cai *et al.*, "A well-mixed phase formed by two compatible non-fullerene acceptors enables ternary organic solar cells with efficiency over 18.6%," *Advanced Materials*, vol. 33, no. 33, p. 2101733, 2021. https://doi.org/10.1002/adma.202101733

[107] Y. Chen, M. Zhang, F. Li, and Z. Yang, "Recent progress in perovskite solar cells: Status and future," *Coatings*, vol. 13, no. 3, p. 644, 2023. https://doi.org/10.3390/coatings13030644

[108] W.-Q. Wu, D. Chen, R. A. Caruso, and Y.-B. Cheng, "Recent progress in hybrid perovskite solar cells based on n-type materials," *Journal of Materials Chemistry A*, vol. 5, no. 21, pp. 10092-10109, 2017.

[109] Z. Arshad *et al.*, "Magnesium doped TiO2 as an efficient electron transport layer in perovskite solar cells," *Case Studies in Thermal Engineering*, vol. 26, p. 101101, 2021. https://doi.org/10.1016/j.csite.2021.101101

[110] R. Xu *et al.*, "Enhanced performance of planar perovskite solar cells using Ce-doped TiO2 as electron transport layer," *Journal of Materials Science*, vol. 55, no. 14, pp. 5681-5689, 2020. https://doi.org/10.1007/s10853-020-04409-9

[111] A. Peter Amalathas, L. Landova, B. Conrad, and J. Holovsky, "Concentration-dependent impact of alkali Li metal doped mesoporous TiO2 electron transport layer on the performance of CH3NH3PbI3 perovskite solar cells," *The Journal of Physical Chemistry C*, vol. 123, no. 32, pp. 19376-19384, 2019.

[112] X. Liu, Z. Wu, Y. Zhang, and C. Tsamis, "Low temperature Zn-doped TiO2 as electron transport layer for 19% efficient planar perovskite solar cells," *Applied Surface Science*, vol. 471, pp. 28-35, 2019. https://doi.org/10.1016/j.apsusc.2018.11.237

[113] S. Sandhu *et al.*, "Micro structurally engineered hysteresis-free high efficiency perovskite solar cell using Zr-doped TiO2 electron transport layer," *Ceramics International*, vol. 47, no. 10, Part A, pp. 14665-14672, 2021. https://doi.org/10.1016/j.ceramint.2021.01.187

[114] J.-B. Wu, C. Zhen, and G. Liu, "Photo-assisted Cl doping of SnO2 electron transport layer for hysteresis-less perovskite solar cells with enhanced efficiency," *Rare Metals*, vol. 41, no. 2, pp. 361-367, 2022. https://doi.org/10.1007/s12598-021-01812-2

[115] J. Tian, J. Zhang, X. Li, B. Cheng, J. Yu, and W. Ho, "Low-temperature-processed Zr/F co-doped SnO2 electron transport layer for high-efficiency planar perovskite solar cells," *Solar RRL*, vol. 4, no. 6, p. 2000090, 2020. https://doi.org/10.1002/solr.202000090

[116] Q. Liu *et al.*, "Effect of tantalum doping on SnO2 electron transport layer via low temperature process for perovskite solar cells," *Applied Physics Letters*, vol. 115, no. 14, 2019.

[117] Z. Arshad *et al.*, "Enhanced charge transport characteristics in zinc oxide nanofibers via Mg2+ doping for electron transport layer in perovskite solar cells and antibacterial textiles," *Ceramics International*, vol. 48, no. 17, pp. 24363-24371, 2022. https://doi.org/10.1016/j.ceramint.2022.05.018

[118] Z. Pang *et al.*, "Hydrophobic PbS QDs layer decorated ZnO electron transport layer to boost photovoltaic performance of perovskite solar cells," *Chemical Engineering Journal*, vol. 439, p. 135701, 2022. https://doi.org/10.1016/j.cej.2022.135701

[119] X. Zhou *et al.*, "Metal–organic framework-derived n-rich porous carbon as an auxiliary additive of hole transport layers for highly efficient and long-term stable perovskite solar cells," *Solar RRL*, vol. 4, no. 3, p. 1900380, 2020. https://doi.org/10.1002/solr.201900380

[120] W. Cao *et al.*, "Redox engineering of spiro-OMeTAD based hole transport layer enabled by ultrathin Co(III)-grafted carbon nitride nanosheets for stable perovskite solar cells," *Nano Energy*, vol. 104, p. 107924, 2022. https://doi.org/10.1016/j.nanoen.2022.107924

[121] Q. Du *et al.*, "Spiro-OMeTAD: Sb2S3 hole transport layer with triple functions of overcoming lithium salt aggregation, long-term high conductivity, and defect passivation for perovskite solar cells," *Solar RRL*, vol. 5, no. 11, p. 2100622, 2021. https://doi.org/10.1002/solr.202100622

[122] X. Zheng *et al.*, "Organic-inorganic hybrid hole transport layers with SnS doping boost the performance of perovskite solar cells," *Journal of Energy Chemistry*, vol. 68, pp. 637-645, 2022. https://doi.org/10.1016/j.jechem.2021.11.034

[123] J. Zheng *et al.*, "Perovskite solar cells employing a PbSO4 (PbO) 4 quantum dot-doped spiro-OMeTAD hole transport layer with an efficiency over 22%," *ACS Applied Materials & Interfaces*, vol. 14, no. 2, pp. 2989-2999, 2022.

[124] W. Han *et al.*, "Recent progress of inverted perovskite solar cells with a modified PEDOT: PSS hole transport layer," *ACS Applied Materials & Interfaces*, vol. 12, no. 44, pp. 49297-49322, 2020.

[125] X. Yang *et al.*, "Boosting performance of inverted perovskite solar cells by diluting hole transport layer," *Nanomaterials*, vol. 12, no. 22, p. 3941, 2022. https://doi.org/10.3390/nano12223941

[126] H. Elbohy *et al.*, "Tuning hole transport layer using urea for high-performance perovskite solar cells," *Advanced Functional Materials*, vol. 29, no. 47, p. 1806740, 2019. https://doi.org/10.1002/adfm.201806740

[127] W. Hu *et al.*, "High open-circuit voltage of 1.134 V for inverted planar perovskite solar cells with sodium citrate-doped PEDOT: PSS as a hole transport layer," *ACS Applied Materials & Interfaces*, vol. 11, no. 24, pp. 22021-22027, 2019.

[128] L. Xu *et al.*, "Inverted perovskite solar cells employing doped NiO hole transport layers: A review," *Nano Energy*, vol. 63, p. 103860, 2019. https://doi.org/10.1016/j.nanoen.2019.103860

[129] P.-H. Lee, B.-T. Li, C.-F. Lee, Z.-H. Huang, Y.-C. Huang, and W.-F. Su, "High-efficiency perovskite solar cell using cobalt doped nickel oxide hole transport layer fabricated by NIR process," *Solar Energy Materials and Solar Cells*, vol. 208, p. 110352, 2020. https://doi.org/10.1016/j.solmat.2019.110352

[130] M. Chen *et al.*, "Homogeneous doping of entire perovskite solar cells via alkali cation diffusion from the hole transport layer," *Journal of Materials Chemistry A*, vol. 9, no. 14, pp. 9266-9271, 2021.

[131] C. Chen *et al.*, "Perovskite solar cells based on screen-printed thin films," *Nature*, vol. 612, no. 7939, pp. 266-271, 2022. https://doi.org/10.1038/s41586-022-05346-0

[132] Z. Li *et al.*, "Ink engineering of inkjet printing perovskite," *ACS Applied Materials & Interfaces*, vol. 12, no. 35, pp. 39082-39091, 2020.

[133] X. Jiao *et al.*, "Anion-exchange assisted sequential deposition for stable and efficient FAPbI3-based perovskite solar cells," *Chemical Engineering Journal*, vol. 452, p. 139326, 2023. https://doi.org/10.1016/j.cej.2022.139326

[134] J. Li *et al.*, "20.8% slot-die coated MAPbI3 perovskite solar cells by optimal DMSO-content and age of 2-ME based precursor inks," *Advanced Energy Materials*, vol. 11, no. 10, p. 2003460, 2021. https://doi.org/10.1002/aenm.202003460

[135] Y. Choi *et al.*, "Toward all-vacuum-processable perovskite solar cells with high efficiency, stability, and scalability enabled by fluorinated spiro-OMeTAD through thermal evaporation," *Solar RRL*, vol. 5, no. 9, p. 2100415, 2021. https://doi.org/10.1002/solr.202100415

[136] J.-W. Lee *et al.*, "Vapor-assisted ex-situ doping of carbon nanotube toward efficient and stable perovskite solar cells," *Nano Letters*, vol. 19, no. 4, pp. 2223-2230, 2018.

[137] D. Hughes *et al.*, "Proton radiation hardness of perovskite solar cells utilizing a mesoporous carbon electrode," *Energy Technology*, vol. 9, no. 12, p. 2100928, 2021. https://doi.org/10.1002/ente.202100928

[138] X. Zhao, C. Xu, X. Wang, J. Guo, and M. Wu, "Construction of multilevel network structured carbon nanofiber counter electrode and back interface engineering in all inorganic HTL–free perovskite solar cells," *Colloids and Surfaces A: Physicochemical and Engineering Aspects*, vol. 648, p. 129420, 2022. https://doi.org/10.1016/j.colsurfa.2022.129420

[139] G. A. Sepalage *et al.*, "Can laminated carbon challenge gold? Toward universal, scalable, and low-cost carbon electrodes for perovskite solar cells," *Advanced Materials Technologies*, vol. 7, no. 6, p. 2101148, 2022. https://doi.org/10.1002/admt.202101148

[140] M. Guo *et al.*, "Composite electrode based on single-atom Ni doped graphene for planar carbon-based perovskite solar cells," *Materials & Design*, vol. 209, p. 109972, 2021. https://doi.org/10.1016/j.matdes.2021.109972

[141] T. A. Chowdhury, M. A. B. Zafar, M. S.-U. Islam, M. Shahinuzzaman, M. A. Islam, and M. U. Khandaker, "Stability of perovskite solar cells: issues and prospects," *RSC Advances*, vol. 13, no. 3, pp. 1787-1810, 2023.

[142] P. Cheng and X. Zhan, "Stability of organic solar cells: challenges and strategies," *Chemical Society Reviews*, vol. 45, no. 9, pp. 2544-2582, 2016.

[143] A. Agresti, S. Pescetelli, Y. Busby, and T. Aernouts, "Thermally Induced Fullerene Domain Coarsening Process in Organic Solar Cells," *IEEE Transactions on Electron Devices*, vol. 66, no. 1, pp. 678-688, 2019. https://doi.org/10.1109/TED.2018.2880760

[144] P. Sommer-Larsen, M. Jørgensen, R. R. Søndergaard, M. Hösel, and F. C. Krebs, "It is all in the pattern—high-efficiency power extraction from polymer solar cells through high-voltage serial connection," *Energy Technology*, vol. 1, no. 1, pp. 15-19, 2013. https://doi.org/10.1002/ente.201200055

[145] C. Bruner, F. Novoa, S. Dupont, and R. Dauskardt, "Decohesion kinetics in polymer organic solar cells," *ACS Applied Materials & Interfaces*, vol. 6, no. 23, pp. 21474-21483, 2014.

[146] M. Ghasemi *et al.*, "Delineation of thermodynamic and kinetic factors that control stability in non-fullerene organic solar cells," *Joule*, vol. 3, no. 5, pp. 1328-1348, 2019. https://doi.org/10.1016/j.joule.2019.03.020

[147] N. Li *et al.*, "Abnormal strong burn-in degradation of highly efficient polymer solar cells caused by spinodal donor-acceptor demixing," *Nature Communications*, vol. 8, no. 1, p. 14541, 2017. https://doi.org/10.1038/ncomms14541

[148] T. Wu *et al.*, "Efficient and stable tin-based perovskite solar cells by introducing π-conjugated Lewis base," *Science China Chemistry*, vol. 63, no. 1, pp. 107-115, 2020. https://doi.org/10.1007/s11426-019-9653-8

[149] T. Nakamura *et al.*, "Sn(IV)-free tin perovskite films realized by in situ Sn(0) nanoparticle treatment of the precursor solution," *Nature Communications*, vol. 11, no. 1, p. 3008, 2020. https://doi.org/10.1038/s41467-020-16726-3